Journal of Medicinal Chemistry

Article

pubs.acs.org/jmc

IspC as Target for Antiinfective Drug Discovery: Synthesis, Enantiomeric Separation, and Structural Biology of Fosmidomycin Thia Isosters

Andrea Kunfermann,[†,#] Claudia Lienau,[‡,#] Boris Illarionov,[§] Jana Held,[∥] Tobias Gräwert,[§] Christoph T. Behrendt,[‡] Philipp Werner,[§] Saskia Hähn,[‡] Wolfgang Eisenreich,[†] Ulrich Riederer,[⊥] Benjamin Mordmüller,[∥] Adelbert Bacher,[§] Markus Fischer,[§] Michael Groll,[†] and Thomas Kurz*[,‡]

[†]Center for Integrated Protein Science Munich, Lehrstuhl für Biochemie, Technische Universität München, Lichtenbergstrasse 4, 85747 Garching, Germany

[‡]Institut für Pharmazeutische und Medizinische Chemie, Heinrich Heine Universität Düsseldorf, Universitätsstrasse 1, 40225 Düsseldorf, Germany

[§]Hamburg School of Food Science, Universität Hamburg, Grindelallee 117, 20146 Hamburg, Germany

[∥]Institut für Tropenmedizin, Eberhard Karls Universität Tübingen, Wilhelmstrasse 27, 72074 Tübingen Germany

[⊥]Institut für Pharmazie, Universität Hamburg, Bundesstrasse 45, 20146 Hamburg, Germany

Supporting Information

ABSTRACT: The emergence and spread of multidrug-resistant pathogens are widely believed to endanger human health. New drug targets and lead compounds exempt from cross-resistance with existing drugs are urgently needed. We report on the synthesis and properties of "reverse" thia analogs of fosmidomycin, which inhibit the first committed enzyme of a metabolic pathway that is essential for the causative agents of tuberculosis and malaria but is absent in the human host. Notably, IspC displays a high level of enantioselectivity for an α-substituted fosmidomycin derivative.

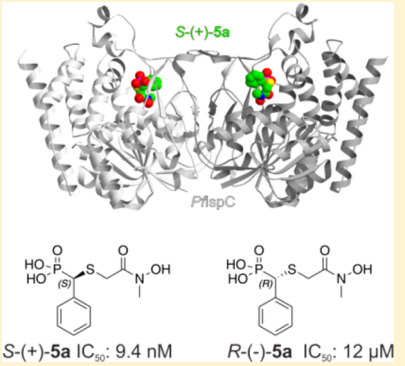

INTRODUCTION

The discussion on the current and future management of malaria, a dominant cause of morbidity and mortality, is characterized by apparently antipodal points of view. Optimistic speculation about the feasibility of eradication coexists with the actual problem of progressing resistance against most or all available drugs and the paucity of recent pharmacological innovation.[1−4]

Fosmidomycin (**1**), a phosphonate antibiotic with a hydroxamate pharmacophore that was originally isolated from *Streptomyces lavendulae*,[5,6] is known to have antibacterial and herbicidal activity and was more recently shown to be active against the *Plasmodium* species causing malaria.[7,8] Its molecular target, IspC, catalyzes the first committed step in the non-mevalonate isoprenoid biosynthesis pathway that is essential in *Plasmodium* spp. but absent in mammals (Scheme 1).[9,10] **1** can cure human malaria and has a favorable toxicity profile but has shortcomings with regard to pharmacokinetic aspects, which prompted structural modifications in several laboratories.[11−27] Also of note, **1** and its analogs are expected to be exempt from target-related toxicity and from cross-resistance with established antimalarials and may even be able to target the malaria liver stages that are insufficiently addressed by current antimalarials.[28,29] We report the synthesis of thia isosters of reversed hydroxamic acid analogs of **1** and their enzymatic, antiparasite, and structural biology features. Furthermore, we show that IspC has a high degree of enantioselectivity for a reverse α-aryl derivative of **1**.

RESULTS AND DISCUSSION

Chemistry. The retrosynthetic analysis of the target structures **5a−e** and **7a−c** suggested α-mercaptophosphonates (**3a−e**), 2-chloro-*N*-hydroxyacetamide, and 2-chloro-*N*-hydroxy-*N*-methylacetamide as suitable building blocks. The alkylating reagents 2-chloro-*N*-hydroxyacetamide and 2-chloro-*N*-hydroxy-*N*-methylacetamide were obtained by published procedures.[30,31] Previously unreported α-mercaptophosphonates **3b−d** were accessible according to a known procedure developed for the preparation of building block **3a**.[32] S-Alkylation of α-mercaptophosphonates (**3a−e**) with 2-

Received: August 13, 2013

   dx.doi.org/10.1021/jm4012559 | J. Med. Chem. XXXX, XXX, XXX−XXX

Scheme 1. Fosmidomycin and Reverse IspC Inhibitors

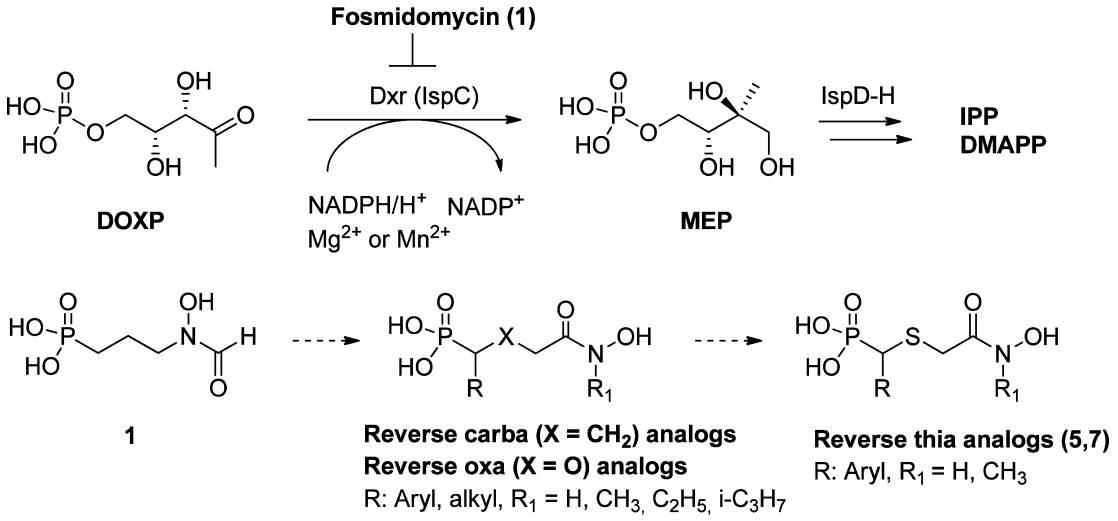

Scheme 2. Synthesis of Fosmidomycin Thia Isosters[a]

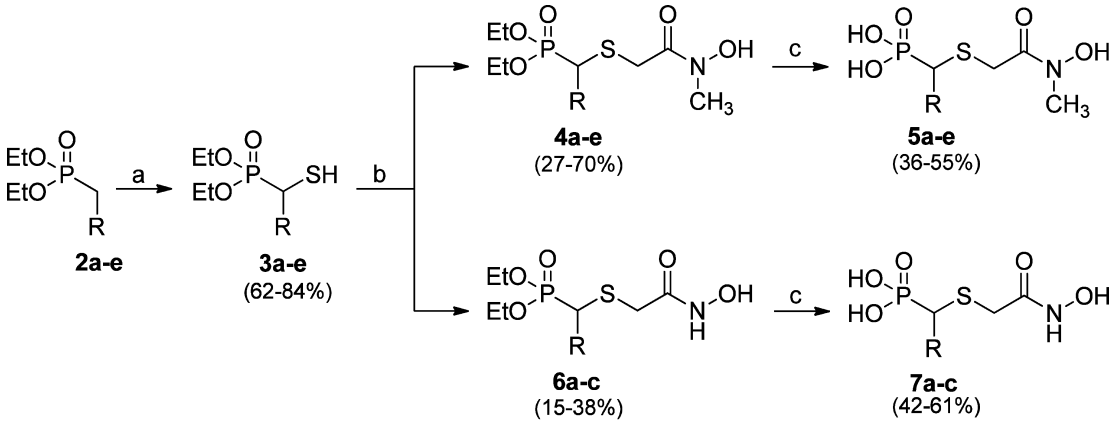

a: R = Ph; **b**: R = 3,4-F-Ph; **c**: R = 3,4-Cl-Ph; **d**: R = naphthalene-1-yl; **e**: R = 4-CH_3-Ph

[a]Reagents and conditions: (a) (1) *n*-BuLi, S, THF, −78 °C, 1 h; (2) −20 °C, THF, 1 h; (3) rt, THF, 1 h. (b)**4a−e**: 2-chloro-*N*-hydroxy-*N*-methylacetamide, DMF, Na_2CO_3, 0 °C → rt. **6a−c**: 2-chloro-*N*-hydroxyacetamide, DMF, Na_2CO_3, 0 °C → rt. (c) (1) TMSBr, CH_2Cl_2, 0 °C, 1 h; (2) CH_2Cl_2, rt, 47 h; (3) THF/H_2O, rt, 45 min.

chloro-*N*-hydroxyacetamides afforded partially protected intermediates **4a−e** and **6a−c** (Scheme 2). Deprotection of their respective phosphonate moieties by treatment with TMSBr afforded the racemic thia analogs **5a−e** and **7a−c** as solids or oils.[33]

Biological Evaluation. Inhibition of IspC from *Plasmodium falciparum* (*Pf*IspC) by thia analogs **5** and **7** was monitored using a photometric assay. IC_{50} values for inhibition of *Pf*IspC and drug sensitivity assay for two different *P. falciparum* strains were in the low nanomolar to micromolar range (Tables 1 and 2 and Supporting Information Figure S1). Typical dose−response curves are shown in Figure 1. In parallel with earlier findings, the *N*-methyl substituted hydroxamates **5** showed lower IC_{50} values than the respective unsubstituted hydroxamic acids **7**.[21,34] Recently we reported reverse carba and oxa analogs of **1** that act as potent inhibitors of IspC and of *P. falciparum* growth.[20,21,35]

In order to unequivocally establish the generic impact of sulfur, oxygen, or methylene in the β-position of α-phenylated reverse derivatives of **1**, the inhibitory activity of small compound libraries comprising isosteric sets of thia, oxa, and carba analogs were determined using IspC orthologs from *Escherichia coli* (*Ec*IspC), *Mycobacterium tuberculosis* (*Mt*IspC), and *P. falciparum*. (See Tables 1 and 2 for an overview of all IC_{50} values.) By comparison with the carba compounds, the thia isosters show increased inhibition (by more than a factor of 10) for IspC proteins of bacterial origin (black ellipse, Figure 2a) but decreased inhibition for *Pf*IspC (red ellipse, Figure 2a). The oxa isosters were less potent inhibitors than the cognate carba compounds for all enzymes under study (red and dashed ellipses, Figure 2a). The correlation between inhibition of IspC protein and of *P. falciparum* blood stages is illustrated in Figure 2b and Figure 2c. One cannot observe a perfect match between activity against the enzyme and against the parasite in vitro. Consistently, the IC_{50} values of the isolated enzyme are lower than the IC_{50} values for parasite growth. This is derived from the fact that the compounds must penetrate several membranes in order to reach the site of IspC in the apicoplast (the

dx.doi.org/10.1021/jm4012559 | J. Med. Chem. XXXX, XXX, XXX−XXX

Table 1. IC_{50} Values of Thia Analogs 5 and 7 versus IspC of *Escherichia coli*, *Mycobacterium tuberculosis*, and *P. falciparum*[d]

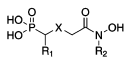	*Ec*IspC[a] IC_{50} [nM]			*Mt*IspC[a] IC_{50} [nM]			*Pf*IspC[a] IC_{50} [nM]		
X =	S	O	C	S	O	C	S	O	C
R_1 = Ph R_2 = CH_3	**5a** 8.2 ± 0.8	**5aO** 940 ± 50	**5aC** 243 ± 30	**5a** 280 ± 30	**5aO** 16000 ± 1000	**5aC** 2000 ± 100	**5a** 24 ± 2	**5aO** 37 ± 2	**5aC** 3.1 ± 0.3
R_1 = 3,4-F-Ph R_2 = CH_3	**5b*** 8.5 ± 1	**5bO** 240 ± 10	**5bC** 117 ± 7	**5b** 42 ± 2	**5bO** 4600 ± 200	**5bC** 770 ± 60	**5b** 14 ± 1	**5bO** 12 ± 1	**5bC** 3.4 ± 0.4
R_1 = 3,4-Cl-Ph R_2 = CH_3	**5c** 5.9 ± 0.6	**5cO** 200 ± 20	208 ± 16	**5c*** 9.2 ± 0.6	**5cO** 1600 ± 100	280 ± 30	**5c** 4.5 ± 0.4	**5cO** 14 ± 1	2.8 ± 0.4
R_1 = naphthalene-1-yl R_2 = CH_3	**5d** 140 ± 10	**5dO** 4600 ± 300	3830 ± 170	**5d*** 550 ± 10	**5dO** 15000 ± 1000	13000 ± 1000	**5d*** 9.8 ± 0.9	**5dO** 39 ± 4	9.4 ± 1.3
R_1 = 4-CH_3-Ph R_2 = CH_3	**5e** 33 ± 9	**5eO** 320 ± 20	286 ± 19	**5e** 110 ± 10	**5eO** 4000 ± 200	1800 ± 100	**5e** 18 ± 4	**5eO** 25 ± 3	14 ± 2
R_1 = Ph R_2 = H	**7a*** 600 ± 90	20000 ± 2000	592 ± 25	**7a*** 15000 ± 1000	466000 ± 60000	14000 ± 1000	**7a** 110 ± 20	1500 ± 100	12 ± 3
R_1 = 3,4-F-Ph R_2 = H	**7b*** 77 ± 6	49000 ± 2000	178 ± 20	**7b*** 1700 ± 100	> 500000	3400 ± 300	**7b** 15 ± 2	3900 ± 200	3.9 ± 0.4
R_1 = 3,4-Cl-Ph R_2 = H	**7c** 44 ± 2	n.s.	n.s.	**7c*** 720 ± 50	n.s.	n.s.	**7c** 200 ± 10	n.s.	n.s.
Fosmidomycin	221 ± 14.4[b]			230 ± 20			160 ± 20[c]		

[a]Enzyme assay. Values were calculated from at least eight data points. In general two to three independent determinations have been performed.[36,37] The asterisk (*) indicates single determination. [b]IC_{50} value according to ref 20. [c]IC_{50} value according to ref 35. [d]n.s.: not synthesized.

Table 2. IC_{50} Values of Thia Analogs 5 and 7 versus *Plasmodium* Strains 3D7 and Dd2[c]

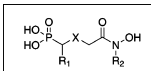	*Pf*3D7[a] IC_{50} [nM]			*Pf*Dd2[a] IC_{50} [nM]		
X =	S	O	C	S	O	C
R_1 = Ph R_2 = CH_3	**5a** 30	**5aO** 1200	**5aC** 90	**5a** 75	**5aO** 700	**5aC** 74
R_1 = 3,4-F-Ph R_2 = CH_3	**5b** 111	**5bO** 540	**5bC** 122	**5b** 88	**5bO** 130	**5bC** 40
R_1 = 3,4-Cl-Ph R_2 = CH_3	**5c** 91	**5cO** 240	n.d.	**5c** 85	**5cO** 140	n.d.
R_1 = naphthalene-1-yl R_2 = CH_3	**5d** 380	**5dO** 520	n.d.	**5d** 510	**5dO** 350	n.d.
R_1 = 4-CH_3-Ph R_2 = CH_3	**5e** 111	**5eO** 180	n.d.	**5e** 95	**5eO** 190	n.d.
R_1 = Ph R_2 = H	**7a** 2900	> 50000	400	**7a** 3770	n.d.	570
R_1 = 3,4-F-Ph R_2 = H	**7b** 160	> 50000	75	**7b** 330	n.d.	65
R_1 = 3,4-Cl-Ph R_2 = H	**7c** 540	n.s.	n.s.	**7c** 870	n.s.	n.s.
Fosmidomycin	880[b]			810[b]		

[a]In vitro assay. Values are the mean of two independent double determinations. [b]IC_{50} value according to ref 35. [c]n.d.: not determined. n.s.: not synthesized.

membranes of the erythrocyte and the parasitophorous vacuole, the outer membrane of the parasite cell, and four membranes of the apicoplast).[38] In agreement with the enzyme assays, the *N*-methyl substituted derivatives **5** also showed higher inhibitory

dx.doi.org/10.1021/jm4012559 | J. Med. Chem. XXXX, XXX, XXX–XXX

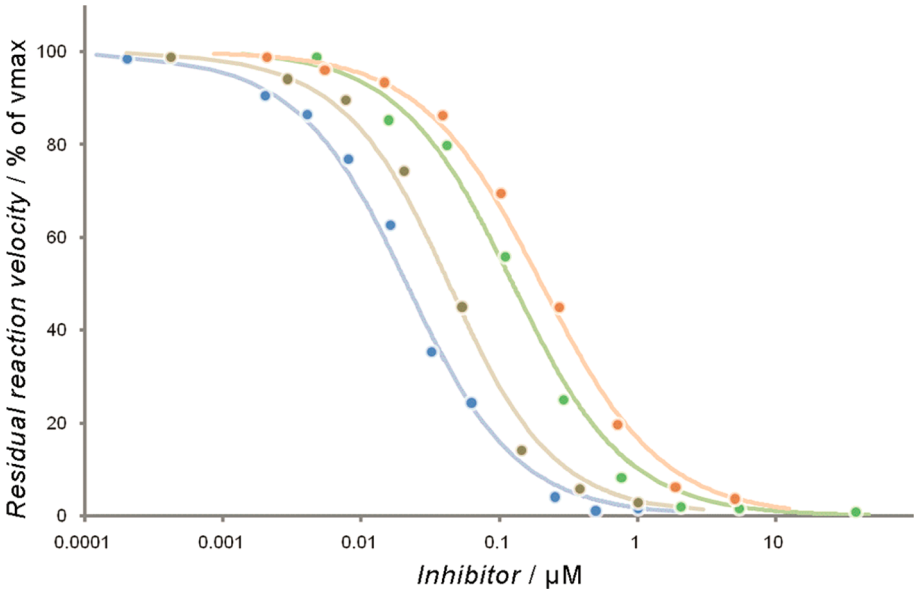

Figure 1. Inhibition of *Pf*IspC by compounds **5a** (blue), **7c** (brown), **7a** (green), **7b** (orange): residual reaction velocity vs inhibitor concentration.

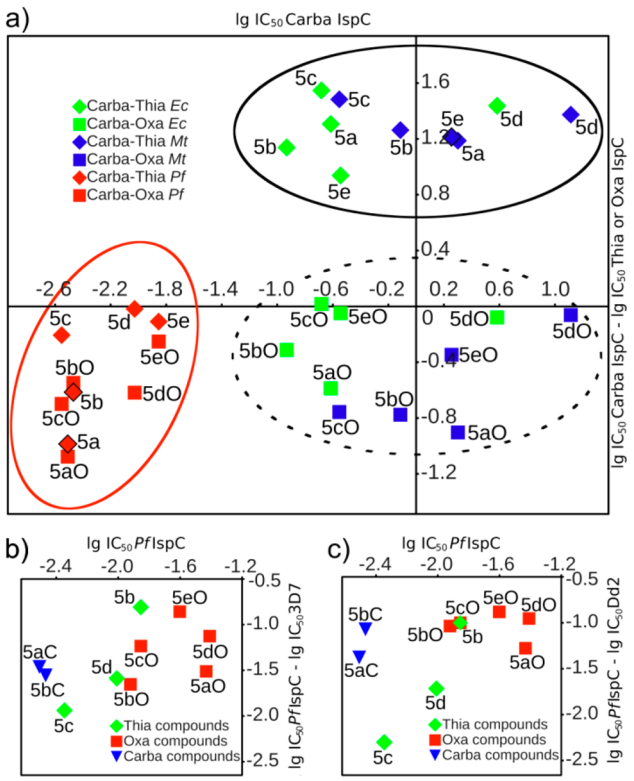

Figure 2. (a) Inhibition of IspC orthologs by minilibraries of carba, oxa, and thia analogs. Abscissa is the log IC_{50} of carba compound. Ordinate is the activity gain with respect to loss caused by sulfur and with respect to oxygen in the β-position. The sulfur isosters show increased inhibition for *Ec*IspC and *Mt*IspC (black ellipse) but decreased inhibition for *Pf*IspC (red ellipse). The oxa isosters exhibit decreased inhibition throughout (red and dashed ellipses). (b, c) Enzyme inhibition compared to inhibition of two different *P. falciparum* strains: (b) strain 3D7; (c) strain Dd2. Abscissa is the IC_{50} for *Pf*IspC. Ordinate is the difference of log IC_{50} (enzyme) and log IC_{50} (parasite proliferation). "C" and "O" after compound numbers designate carba and oxa isosters, respectively. See Tables 1 and 2 for details on the IC_{50} values.

activity toward strains 3D7 and Dd2 than the free hydroxamic acids **7**. The most active thia analog (**5a**) showed an IC_{50} value of 30 nM against the *Plasmodium* 3D7 strain. Differences in membrane permeability of the compounds might also be the reason for deviating results between activities against the *Pf*IspC and the whole parasite in vitro, explaining the correlation discrepancy of the assays.

Next, we determined the three-dimensional structure of *Pf*IspC in complex with Mn^{2+}, NADPH, and **5a** at a resolution of 2.0 Å (PDB code 4KP7, R_{free} = 24.9%), applying Patterson search calculations with the coordinates of *Pf*IspC (PDB code 3AU8[39]) as starting model. Details on data collection and refinement statistics can be found in Table 4 in the Experimental Section. The overall structure is similar to previously reported *Pf*IspC structures (root-mean-square deviation of C_α of <0.6 Å for PDB code 3AU8). The reversed hydroxamate moiety of the bound **5a** chelates the metal ion (Mn^{2+}), which is also coordinated by Asp231, Glu233, and Glu315 of the enzyme (Figure 3a and Figure 3b). In contrast to *Ec*IspC, where the coordination of Mn^{2+} is octahedral because of an additional water molecule, the metal ion is 5-fold coordinated in the case of *Pf*IspC and *Mt*IspC complex structures (see also Supporting Information Figures S2−S4). The phosphonate group forms hydrogen bonds with Ser269, Ser270, Ser306, Asn311, Lys312, and two water molecules. Apart from Ser269, the amino acids involved in direct contact with the ligand are strictly conserved (Supporting Information Figure S5). The loop that covers the ligand is well-defined, whereas it is typically disordered in previously reported IspC structures.[40] The Trp296 and Met298 residues in this region further stabilize the bound ligand by hydrophobic interactions. As shown by the Connolly surface representation (Figure 3c), **5a**, Mn^{2+}, and two water molecules are enclosed in the active site cavity. The loop region over the active site is highly mobile and can thereby accept more bulky residues like the phenyl group in **5a** or the naphthyl group in **5d**.

As seen in the complex structure, the sulfur atom of the ligand is involved in hydrophobic interactions with the strictly conserved Met298. In contrast, the oxygen atom at the β-methylene position would have a repulsive effect with the sulfur

dx.doi.org/10.1021/jm4012559 | J. Med. Chem. XXXX, XXX, XXX−XXX

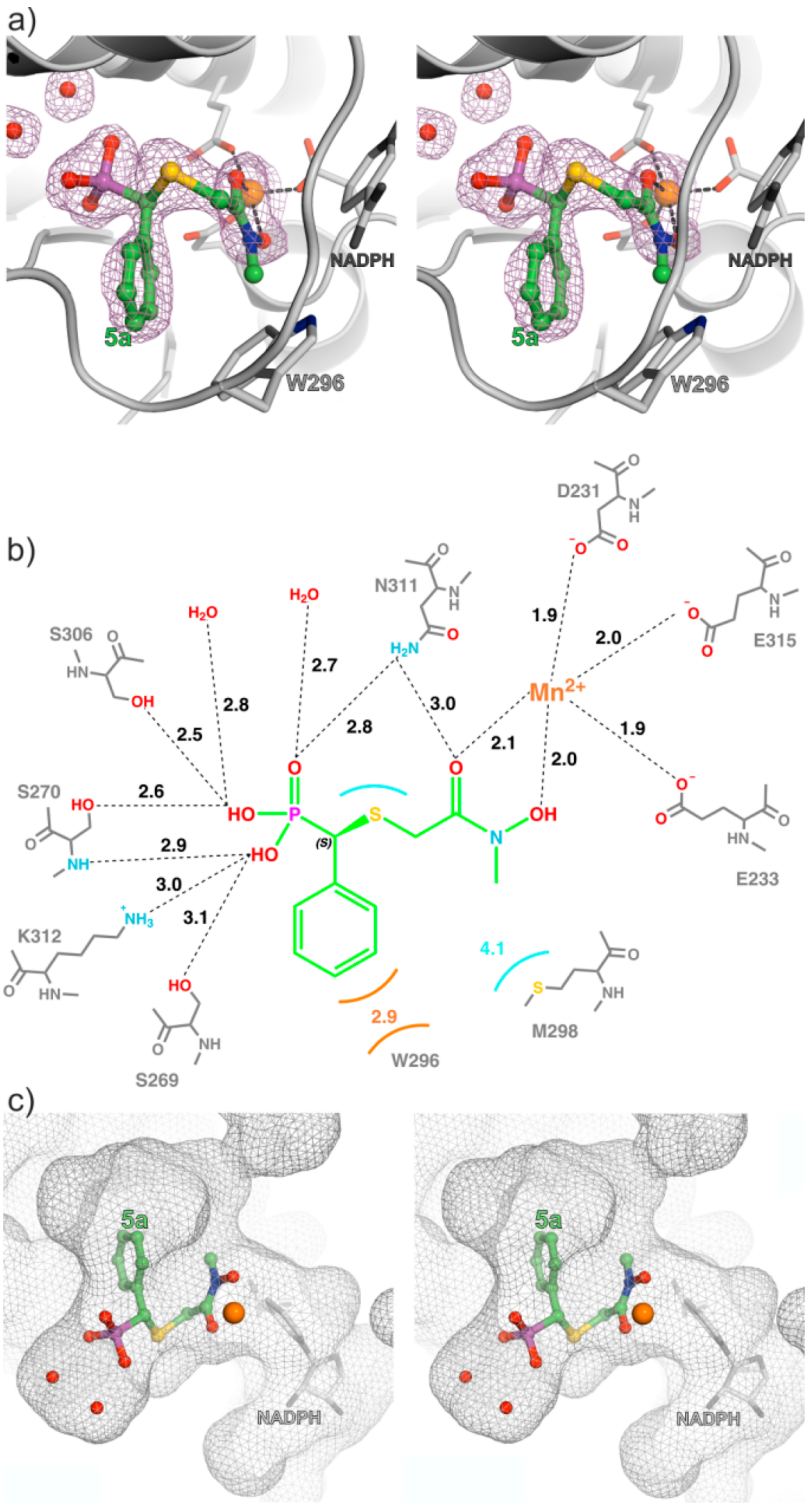

Figure 3. (a) Stereoview of **5a** (green) bound to the active site of *Pf*IspC (gray) at 2.0 Å resolution. NADPH is shown in gray, Mn^{2+} in orange, and the electron density (purple mesh) is displayed at 1.0σ contour level. Ligands have been excluded prior to phase calculating. (b) Interactions of amino acid residues in contact with **5a** and Mn^{2+}. Distances are given in Å. van der Waals interactions are indicated by colored curves. (c) Stereoview of the Connolly surface representation of the active site cavity.

atom of Met298. This is in good agreement with the corresponding IC_{50} values. The carbon atom at this position is not in contact with the protein. Since the IC_{50} values for the thia analogs are significantly lower than for the carba derivatives, it can be assumed that the increased flexibility caused by the sulfur introduction facilitates the binding process of the ligand into the active site cavity. This effect can be clearly seen for *Ec*IspC as well as *Mt*IspC. However, this correlation is less distinctive regarding *Pf*IspC.

Whereas cocrystallization had been performed with the racemic inhibitor, the omit map clearly illustrates that the enzyme selectively binds the *S*-enantiomer. Notably, the high

dx.doi.org/10.1021/jm4012559 | *J. Med. Chem.* XXXX, XXX, XXX–XXX

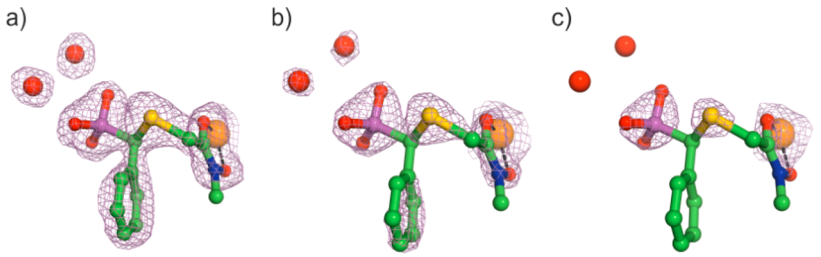

Figure 4. Different contour levels for the electron density map (purple mesh) of *S*-**5a**/*Pf*IspC/Mn/NADPH calculated at 2.0 Å resolution. Density is displayed at (a) 1.0σ, (b) 2.0σ, and (c) 3.0σ contour level.

contrast provided by the electron-rich sulfur strongly supports the chirality assignment. To illustrate the strength of the crystallographic information, different contour levels for the electron density of the sulfur atom are provided in Figure 4. In previous crystallographic studies using several IspC orthologs in complex with α-phenylated derivatives of **1**, *S*-configuration of the enzyme-bound ligands had been the preferred interpretation,[21,22,41] but a definitive chirality assignment had not been possible up to now.

In order to quantitatively assess the enantioselectivity toward IspC, the enantiomers of **5a** were separated by chiral HPLC (with ee > 99.9%). The apparent IC_{50} values of the (+)- and (−)-enantiomers measured against *Pf*IspC are 9.4 nM (+) and >10 μM (−), respectively (Table 3, Figure 5), a similar range that has also been recorded for the bacterial enzymes. On the basis of the kinetic data and the crystallographic complex structure, the more active enantiomer can now be unequivocally assigned as *S*-(+)-**5a**. Thus, because of the strong enantioselectivity, the inhibitory activity of α-substituted derivatives of **1** can be virtually doubled by racemate separation, while undesirable effects can be diminished by the removal of the less active enantiomer.

Table 3. Inhibition of IspC Enzymes of *E. coli*, *M. tuberculosis* and *P. falciparum* by 5a

	IC_{50} [nM][a]		
5a	*Ec*IspC	*Mt*IspC	*Pf*IspC
R-(−)	4000 ± 700	83000 ± 13000	12000 ± 1000
S-(+)	5.1 ± 1.6	120 ± 20	9.4 ± 0.6
racemate	8.2 ± 0.8	280 ± 30	24 ± 2.0

[a]Enzyme assay. Values were calculated from at least eight data points. In general two to three independent determinations have been performed. See Supporting Information Figure S3 and Table S1 for details on the multiple reaction monitoring.

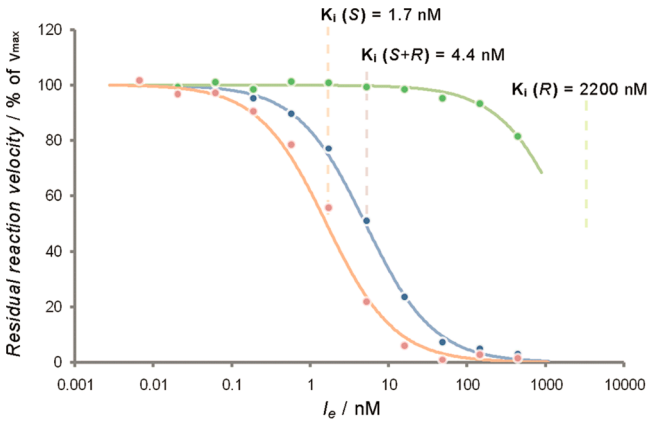

Figure 5. Inhibition of *Pf*IspC by inhibitor **5a**: *S*-(+)-enantiomer, orange; *R*-(−)-enantiomer, green; racemate, blue. I_e is an effective inhibitor concentration, which is calculated according to $I_e = I/(1 + [S]/K_m)$ where I is the inhibitor concentration, $[S]$ is the substrate concentration, and K_m is the Michaelis−Menten constant. At a residual reaction velocity of 50%, I_e is equal to the K_i (inhibition constant) of the inhibitor.

CONCLUSION

In summary, we provided kinetic and crystallographic evidence for the mode of action of a novel type of reverse hydroxamate-based IspC inhibitors. We could show that certain analogs of **1** inhibit IspC with IC_{50} values in the single-digit nanomolar range while inhibiting the parasite growing in human erythrocytes with IC_{50} values in the low nanomolar range. The introduction of a sulfur atom at the β-methylene group of the main chain of the ligands led to an improvement of the IC_{50} values in the cases of *Ec*IspC and *Mt*IspC, compared to the respective carba and oxa ligands. The presented results highlight the more potent inhibitory activity of the *S*-(+)-enantiomer; thus, the long pending question of the stereochemistry of chiral IspC ligands is now clarified. The achievements in the mode of action to block IspC activity might be a helpful guide for the development of more potent chiral inhibitors.

EXPERIMENTAL SECTION

General Procedures. All solvents and chemicals were used as purchased without further purification. The progress of all reactions was monitored on Merck precoated silica gel plates (with fluorescence indicator UV_{254}) using ethyl acetate/*n*-hexane as solvent system. Column chromatography was performed with Fluka silica gel 60 (230−400 mesh ASTM) with the solvent mixtures specified in the corresponding experiment. Spots were visualized by irradiation with ultraviolet light (254 nm). Melting points (mp) were taken in open capillaries on a Stuart melting point apparatus SMP11 and are uncorrected. Proton (^{1}H) and carbon (^{13}C) NMR spectra were recorded on a Bruker Avance 500 (500.13 MHz for ^{1}H; 125.76 MHz for ^{13}C) using DMSO-d_6 as solvent. Chemical shifts are given in parts per million (ppm) (δ relative to residual solvent peak for ^{1}H and ^{13}C). Elemental analysis was performed on a Perkin-Elmer PE 2400 CHN elemental analyzer and a vario MICRO cube elemental analyzer, Elementar Analysensysteme GmbH, Hanau Germany. IR spectra were recorded on a Varian 800 FT-IR Scimitar series. Optical rotation was determined by a Krüss P8000 polarimeter. Specific rotations $[\alpha]_D^{20}$ are given in deg cm^3 g^{-1} dm^{-1}. High-resolution mass spectrometry (HRMS) analysis was performed using a UHR-TOF maXis 4G instrument (Bruker Daltonics, Bremen, Germany). If necessary, the purity was determined by high performance liquid chromatography (HPLC). Purity of all final compounds was 95% or higher. The instrument was an Elite LaChrom system [Hitachi L-2130 (pump) and L-2400 (UV-detector)]. The column was a Phenomenex Luna C-

dx.doi.org/10.1021/jm4012559 | J. Med. Chem. XXXX, XXX, XXX−XXX

18(2), 5 μm particle size (250 mm × 4.6 mm), supported by Phenomenex Security Guard cartridge kit C18 (4.0 mm ×3.0 mm). Chiral HPLC separation of compound **5a** was performed on HP series 1100 (Agilent): column, Chiralcel OZ-H (Chiral Technologies Europe), 5 μm particle size (250 mm × 4.6 mm); eluent A, *n*-heptane; eluent B, propan-2-ol with 0.1% trifluoroacetic acid, isocratic (70:30) with a flow rate of 1 mL min^{-1} and detection at 240 nm; column temperature of 25 °C; injection of 50 μL of 34.3 mM **5a** in *n*-heptane/propan-2-ol (70:30).

Materials. Diethylphosphonates **2a−e**, α-mercaptophosphonates **3a** and **3e**, 2-chloro-*N*-hydroxy-*N*-methylacetamide, and 2-chloro-*N*-hydroxyacetamide have been prepared according to known procedures.[30,31] α-Mercaptophosphonates **3a−e** were synthesized according to the procedure of Mikolajczyk.[32] Compound **3a** has been previously described by Mikolajczyk[32] and compound **3e** by Creary.[42]

Diethyl ((3,4-Difluorophenyl)(mercapto)methyl)-phosphonate (3b). Yellow oil; yield 67% (9.931 g, 33.52 mmol). ^{1}H NMR (500.13 MHz, [D_6]DMSO): δ = 7.57−7.17 (m, 3H), 4.81 (d, ^2J(H,P) = 20.0 Hz, 0.31H, PCH), 4.76 (d, ^2J(H,P) = 19.2 Hz, 0.26H, PCH), 4.59 (d, ^2J(H,P) = 19.7 Hz, 0.21H, PCH), 4.57 (d, ^2J(H,P) = 19.7 Hz, 0.22H, PCH), 4.15−3.99 (m, 2H, $POCH_2$), 3.99−3.76 (m, 2H, $POCH_2$), 3.70−3.64 (m, SH), 1.31−1.14 (m, 3H, CH_3), 1.14−0.97 ppm (m, 3H, CH_3). ^{13}C NMR (125.76 MHz, [D_6]DMSO): δ = 149.84 (m), 147.82 (m), 135.75 (m), 132.36 (m), 132.03 (m), 126.63 (m), 125.70 (m), 118.52 (m), 117.46 (m), 62.90 (m, $POCH_2$), 62.63 (d, ^2J(C,P) = 6.9 Hz, $POCH_2$), 47.85 (d, ^1J(C,P) = 138.6 Hz, PC), 47.67 (d, ^1J(C,P) = 141.3 Hz, PC), 35.33 (d, ^1J(C,P) = 146.2 Hz, PC), 16.24−15.79 ppm (m, CH_3). IR (NaCl): $\tilde{\nu}$ =2985 (s; ν(C−H_{aliph})), 2913 (m; ν(C−H_{aliph})), 2507 (w; ν(S−H)), 1250 (s; ν(P═O)), 1050 (s; ν(P−O)), 1025 cm^{-1} (s; ν(P−O)). HRMS (ESI): *m*/*z* calculated for $C_{11}H_{15}F_2O_3PS$ + H^+ [M + H^+]: 297.052 03. Found: 297.052 15.

Diethyl ((3,4-Dichlorophenyl)(mercapto)methyl)-phosphonate (3c). Yellow oil; yield 62% (10.201 g, 30.99 mmol). ^{1}H NMR (500.13 MHz, [D_6]DMSO): δ = 8.09 (d, *J* = 2.1 Hz, 0.05H), 7.93 (d, *J* = 2.1 Hz, 0.02H), 7.92 (d, *J* = 2.2 Hz, 0.03H), 7.85 (s, 0.04H), 7.83 (s, 0.04H), 7.80−7.77 (m, 0.08H), 7.73−7.61 (m, 1.2H), 7.60−7.48 (m, 0.7H), 7.45−7.31 (m, 0.84H), 5.28 (d, ^2J(H,P) = 20.5 Hz, 0.06H, PCH), 5.04 (d, ^2J(H,P) = 19.8 Hz, 0.1H, PCH), 5.02 (d, ^2J(H,P) = 20.1 Hz, 0.11H, PCH), 4.93 (d, ^2J(H,P) = 20.2 Hz, 0.14H, PCH), 4.88 (d, ^2J(H,P) = 20.1 Hz, 0.33H, PCH), 4.79 (d, ^2J(H,P) = 19.1 Hz, 0.26H, PCH), 4.17−3.79 (m, 4H, $POCH_2$), 1.31−1.15 (m, 3.34H, CH_3), 1.13−0.98 ppm (m, 2.66H, CH_3). ^{13}C NMR (125.76 MHz, [D_6]DMSO): δ = 135.66 (d, ^2J(C,P) = 4.6 Hz), 135.40 (d, ^4J(C,P) = 2.9 Hz), 131.44 (m), 130.70 (m), 129.75 (m), 63.03 (m, $POCH_2$), 62.49 (m, $POCH_2$), 47.61 (d, ^1J(C,P) = 137.5 Hz, PC), 16.05 ppm (m, CH_3). IR (NaCl): $\tilde{\nu}$ =2983 (s; ν(C−H_{aliph})), 2910 (s; ν(C−H_{aliph})), 2562 (w; ν(S−H)), 1251 (s; ν(P═O)), 1028 cm^{-1} (s; ν(P−O)). HRMS (ESI): *m*/*z* calculated for $C_{11}H_{15}Cl_2O_3PS$ + H^+ [M + H^+]: 328.992 93. Found: 328.992 98.

Diethyl (Mercapto(naphthalene-1-yl)methyl)phosphonate (3d). Yellow oil; yield 84% (13.028 g, 41.98 mmol). ^{1}H NMR (500.13 MHz, [D_6]DMSO): δ = 8.30 (s, 1H), 7.95 (d, *J* = 7.6 Hz, 1.20H), 7.88 (d, *J* = 7.9 Hz, 1.80H), 7.64−7.46 (m, 3H), 5.32−5.18 (m, 1H, PCH), 4.19−4.10 (m, 2H, $POCH_2$), 3.87−3.77 (m, 1H, $POCH_2$), 3.70−3.60 (m, 1H, $POCH_2$), 3.59−3.52 (m, SH), 1.25 (t, ^3J(H,H) = 7.0 Hz, 3H, CH_3), 0.85 ppm (t, ^3J(H,H) = 7.0 Hz, 3H, CH_3). ^{13}C NMR (125.76 MHz, [D_6]DMSO): δ = 133.84 (m), 133.24, 130.51 (d, ^3J(C,P) = 7.6 Hz), 128.60, 128.02, 127.08 (m), 126.29 (m), 125.81 (m), 125.26 (m), 123.54 (m), 62.92 (d, ^2J(C,P) = 7.0 Hz, $POCH_2$), 32.23 (m, PC), 31.02 (m, PC), 16.29 (m, CH_3), 15.80 ppm (m, CH_3). IR (NaCl): $\tilde{\nu}$ =2981 (s; ν(C−H_{aliph})), 2517 (w; ν(S−H)), 1249 (s; ν(P═O)), 1051 (s; ν(P−O)), 1024 cm^{-1} (s; ν(P−O)). HRMS (ESI): *m*/*z* calculated for $C_{15}H_{19}O_3PS$ + H^+ [M + H^+]: 311.086 53. Found: 311.086 91.

General Procedure for the Synthesis of Intermediates 4a−e and 6a−c. After purification, compounds **3a−e** were immediately used for the synthesis of **4a−e** and **6a−c**. Under a nitrogen atmosphere, the respective α-mercaptophosphonate **3a−e** (1 equiv, 10 mmol) was dissolved in dry dimethylformamide (10 mL). After addition of Na_2CO_3 (1.25 equiv, 1.32 g, 12.5 mmol) the reaction mixture was cooled to 0 °C. In the case of the preparation of **4a−e**, a solution of 2-chloro-*N*-hydroxy-*N*-methylacetamide (1 equiv, 1.24 g, 10 mmol) in dry dimethylformamide (2 mL) was added dropwise. For the synthesis of **6a−c**, 2-chloro-*N*-hydroxyacetamide (1 equiv, 1.10 g, 10 mmol) in dry dimethylformamide (2 mL) was used as alkylating agent. The reaction mixture was allowed to warm to room temperature and stirred for 2 h while monitoring the progress of the reaction by thin layer chromatography. Ethyl acetate (40 mL) and 1 M hydrochloric acid (10 mL) were added, and the aqueous DMF layer was extracted and separated. Next the aqueous DMF layer was extracted three more times with ethyl acetate (3 × 30 mL). The ethyl acetate was washed with 1 M hydrochloric acid (10 mL), dried over Na_2SO_4, filtered, and evaporated to dryness. The residues were purified by column chromatography on silica gel using ethyl acetate/*n*-hexane (10:90 → 100:0) to give hydroxamic acids **4a−e** and **6b** as white solids and compounds **6a,c** as colorless oils.

Diethyl (((2-Hydroxy(methyl)amino)-2-oxoethyl)thio-(phenyl)methyl)phosphonate (4a). White solid; yield 41% (1.421 g, 4.09 mmol); mp 79 °C. ^{1}H NMR (500.13 MHz, [D_6]DMSO): δ = 10.02 (br s, OH), 7.45−7.39 (m, 2H), 7.38−7.32 (m, 2H), 7.32−7.26 (m, 1H), 4.57 (d, ^2J(H,P) = 19.7 Hz, 1H, PCH), 4.12−3.99 (m, 2H, $POCH_2$), 3.95−3.84 (m, 1H, $POCH_2$), 3.84−3.73 (m, 1H, $POCH_2$), 3.53 (d, ^2J(H,H) = 14.7 Hz, 1H, SCH_2), 3.34 (d, ^2J(H,H) = 14.7 Hz, 1H, SCH_2), 3.06 (s, 3H, NCH_3), 1.22 (t, ^3J(H,H) = 7.0 Hz, 3H, CH_3), 1.04 ppm (t, ^3J(H,H) = 7.0 Hz, 3H, CH_3). ^{13}C NMR (125.76 MHz, [D_6]DMSO): δ = 168.41 (C═O), 135.55 (d, ^2J(C,P) = 4.2 Hz), 129.12 (d, ^3J(C,P) = 6.4 Hz), 128.23, 127.52, 62.50 (d, ^2J(C,P) = 6.9 Hz, $POCH_2$), 62.42 (d, ^2J(C,P) = 6.9 Hz, $POCH_2$), 43.37 (d, ^1J(C,P) = 143.6 Hz, PC), 35.72 (NCH_3), 32.12 (d, ^3J(C,P) = 6.6 Hz, SCH_2), 16.13 (d, ^3J(C,P) = 5.6 Hz, CH_3), 15.92 (d, ^3J(C,P) = 5.5 Hz, CH_3). IR (KBr): $\tilde{\nu}$ =3103 (s; ν(O−H)), 2983 (s; ν(C−H_{aliph})), 2902 (s; ν(C−H_{aliph})), 1650 (s; ν(C═O)), 1209 (s; ν(P═O)), 1042 cm^{-1} (s; ν(P−O)). Elemental analysis calculated (%) for $C_{14}H_{22}NO_5PS$: C 48.41, H 6.38, N 4.03. Found: C 48.58, H 6.51, N 3.87.

Diethyl ((3,4-Difluorophenyl)((2-(hydroxy(methyl)amino)-2-oxoethyl)thio)methyl)phosphonate (4b). White solid; yield 44% (1.691 g, 4.41 mmol); mp 102 °C. ^{1}H NMR (500.13 MHz, [D_6]DMSO): δ = 10.02 (br s, OH), 7.49−7.38 (m, 2H), 7.31−7.23 (m, 1H), 4.64 (d, ^2J(H,P) = 20.3 Hz, 1H, PCH), 4.12−4.04 (m, 2H, $POCH_2$), 3.97−3.89 (m, 1H, $POCH_2$), 3.89−3.82 (m, 1H, $POCH_2$), 3.52 (d, ^2J(H,H) = 14.8 Hz, 1H, SCH_2), 3.38 (d, ^2J(H,H) = 14.9 Hz, 1H, SCH_2), 3.05 (s, 3H, NCH_3), 1.23 (t, ^3J(H,H) = 7.0 Hz, 3H, CH_3), 1.08 ppm (t, ^3J(H,H) = 7.0 Hz, 3H, CH_3). ^{13}C NMR (125.76 MHz, [D_6]DMSO): δ = 168.11 (C═O), 149.75 (m), 147.81 (m), 133.57, 126.09 (m), 117.88 (dd, ^2J(C,F) = 17.5 Hz, ^3J(C,F) = ^3J(C,P) = 6.2 Hz), 117.32 (d, ^2J(C,F) = 17.3 Hz), 62.74 (d, ^2J(C,P) = 7.2 Hz, $POCH_2$), 62.66 (d, ^2J(C,P) = 7.3 Hz, $POCH_2$), 42.49 (d, ^1J(C,P) = 144.1 Hz, PC), 35.72 (NCH_3), 32.37 (d, ^3J(C,P) = 7.6 Hz, SCH_2), 16.12 (d, ^3J(C,P) = 5.7 Hz, CH_3), 15.96 ppm (d, ^3J(C,P) = 5.5 Hz, CH_3). IR (KBr): $\tilde{\nu}$ =3169 (s; ν(O−H)), 2989 (s; ν(C−H_{aliph})), 2910 (s; ν(C−H_{aliph})), 1642 (s; ν(C═O)), 1230 (s; ν(P═O)), 1022 cm^{-1} (s; ν(P−O)). Elemental analysis calculated (%) for $C_{14}H_{20}F_2NO_5PS$: C 43.86, H 5.26, N 3.65. Found: C 44.09, H 5.41, N 3.55.

Diethyl ((3,4-Dichlorophenyl)((2-(hydroxy(methyl)amino)-2-oxoethyl)thio)methyl)phosphonate (4c). White solid; yield 51% (2.119 g, 5.09 mmol); mp 86 °C. ^{1}H NMR (500.13 MHz, [D_6]DMSO): δ = 10.03 (br s, OH), 7.67−7.62 (m, 2H), 7.44−7.39 (m, 1H), 4.67 (d, ^2J(H,P) = 20.5 Hz, 1H, PCH), 4.12−4.03 (m, 2H, $POCH_2$), 3.99−3.83 (m, 2H, $POCH_2$), 3.51 (d, ^2J(H,H) = 14.8 Hz, 1H, SCH_2), 3.40 (d, ^2J(H,H) = 14.9 Hz, 1H, SCH_2), 3.05 (s, 3H, NCH_3), 1.23 (t, ^3J(H,H) = 7.0 Hz, 3H, CH_3), 1.09 ppm (t, ^3J(H,H) = 7.0 Hz, 3H, CH_3). ^{13}C NMR (125.76 MHz, [D_6]DMSO): δ = 168.03 (C═O), 137.14 (d, ^2J(C,P) = 4.2 Hz), 130.81 (d, ^3J(C,P) = 6.5 Hz), 130.73, 130.49, 130.15 (d, ^4J(C,P) = 2.8 Hz), 129.38 (d, ^3J(C,P) = 6.2 Hz), 62.84 (d, ^2J(C,P) = 6.8 Hz, $POCH_2$), 62.70 (d, ^2J(C,P) = 6.9 Hz, $POCH_2$), 42.41 (d, ^1J(C,P) = 143.0 Hz, PC), 35.72 (NCH_3), 32.53 (d, ^3J(C,P) = 7.6 Hz, SCH_2), 16.12 (d, ^3J(C,P) = 5.7 Hz, CH_3), 15.96 ppm (d, ^3J(C,P) = 5.5 Hz, CH_3). IR (KBr): $\tilde{\nu}$ =3184 (s; ν(O−H)),

dx.doi.org/10.1021/jm4012559 | J. Med. Chem. XXXX, XXX, XXX−XXX

2979 (s; ν(C−H_{aliph})), 2916 (s; ν(C−H_{aliph})), 1648 (s; ν(C═O)), 1226 (s; ν(P═O)), 1052 cm^{-1} (s; ν(P−O)). Elemental analysis calculated (%) for $C_{14}H_{20}Cl_2NO_5PS$: C 40.40, H 4.84, N 3.36. Found: C 40.65, H 4.83, N 3.30.

Diethyl (((2-(Hydroxy(methyl)amino)-2-oxoethyl)thio)-(naphthalen-1-yl)methyl)phosphonate (4d). White solid; yield 70% (2.778 g, 6.99 mmol); mp 85 °C. ^{1}H NMR (500.13 MHz, [D_6]DMSO): δ = 10.02 (br s, OH), 8.22 (d, J = 7.6 Hz, 1H), 7.96 (d, J = 7.8 Hz, 1H), 7.89 (d, J = 8.0 Hz, 1H), 7.87−7.81 (m, 1H), 7.62−7.50 (m, 3H), 5.49 (d, ^2J(H,P) = 19.6 Hz, 1H, PCH), 4.13−4.04 (m, 2H, $POCH_2$) 3.90−3.80 (m, 1H, SCH_2), 3.76−3.64 (m, 2H, $POCH_2$), 3.43−3.37 (m, 1H, SCH_2), 3.06 (s, 3H, NCH_3), 1.24−1.17 (m, 3H, CH_3), 0.94−0.86 ppm (m, 3H, CH_3). ^{13}C NMR (125.76 MHz, [D_6]DMSO): δ = 168.60 (C═O), 133.27 (m), 131.66 (m), 131.14 (m), 128.61, 128.08, 127.16 (m), 126.33 (m), 125.78, 125.22, 123.28 (m), 62.56 (d, ^2J(C,P) = 7.0 Hz, $POCH_2$), 37.46 (d, ^1J(C,P) = 147.51 Hz, PC), 35.72 (NCH_3), 32.29 (m, SCH_2), 16.16 (d, ^3J(C,P) = 5.8 Hz, CH_3), 15.80 ppm (d, ^3J(C,P) = 5.7 Hz, CH_3). IR (KBr): $\tilde{\nu}$ =3154 (s; ν(O−H)), 2983 (s; ν(C−H_{aliph})), 2921 (s; ν(C−H_{aliph})), 1651 (s; ν(C═O)), 1225 (s; ν(P═O)), 1020 cm^{-1} (s; ν(P−O)). Elemental analysis calculated (%) for $C_{18}H_{24}NO_5PS$: C 54.40, H 6.09, N 3.52. Found: C 54.52, H 6.14, N 3.47.

Diethyl (((2-(Hydroxy(methyl)amino)-2-oxoethyl)thio)(*p*-tolyl)methyl)phosphonate (4e). White solid; yield 27% (0.979 g, 2.71 mmol); mp 57 °C. ^{1}H NMR (500.13 MHz, [D_6]DMSO): δ = 10.00 (br s, OH), 7.29 (d, ^3J(H,H) = 7.8 Hz, 2H), 7.15 (d, ^3J(H,H) = 7.8 Hz, 2H), 4.52 (d, ^2J(H,P) = 19.6 Hz, 1H, PCH), 4.12−3.97 (m, 2H, $POCH_2$), 3.94−3.84 (m, 1H, $POCH_2$), 3.84−3.72 (m, 1H, $POCH_2$), 3.51 (d, ^2J(H,H) = 14.8 Hz, 1H, SCH_2), 3.30−3.26 (m, 1H, SCH_2), 3.06 (s, 3H, NCH_3), 2.29 (s, 3H, CH_{3arom}), 1.22 (t, ^3J(H,H) = 7.0 Hz, 3H, CH_3), 1.06 ppm (t, ^3J(H,H) = 7.0 Hz, 3H, CH_3). ^{13}C NMR (125.76 MHz, [D_6]DMSO): δ = 168.46 (C═O), 136.71 (d, ^5J(C,P) = 1.9 Hz), 132.38 (d, ^2J(C,P) = 4.5 Hz), 129.00 (d, ^3J(C,P) = 6.4 Hz), 128.79, 62.42 (d, ^2J(C,P) = 7.2 Hz, $POCH_2$), 62.35 (d, ^2J(C,P) = 7.0 Hz, $POCH_2$), 43.06 (d, ^1J(C,P) = 144.2 Hz, PC), 35.71 (NCH_3), 32.00 (d, ^3J(C,P) = 6.5 Hz, SCH_2), 20.60 (CH_{3arom}), 16.13 (d, ^3J(C,P) = 5.6 Hz, CH_3), 15.95 ppm (d, ^3J(C,P) = 5.6 Hz, CH_3). IR (KBr): $\tilde{\nu}$ =3165 (s; ν(O−H)), 2983 (s; ν(C−H_{aliph})), 2921 (s; ν(C−H_{aliph})), 1650 (s; ν(C═O)), 1222 (s; ν(P═O)), 1035 cm^{-1} (s; ν(P−O)). Elemental analysis calculated (%) for $C_{15}H_{24}NO_5PS$: C 49.85, H 6.69, N 3.88. Found: C 49.74, H 6.73, N 3.70.

Diethyl (((2-Hydroxyamino)-2-oxoethyl)thio)(phenyl)-methyl)phosphonate (6a). Colorless oil; yield 15% (0.500 g, 1.50 mmol). ^{1}H NMR (500.13 MHz, [D_6]DMSO): δ = 10.59 (br s, OH), 8.94 (br s, NH), 7.44−7.38 (m, 2H), 7.37−7.34 (m, 2H), 7.31−7.28 (m, 1H), 4.62 (d, ^2J(H,P) = 19.7 Hz, 1H, PCH), 4.11−4.02 (m, 2H, $POCH_2$), 3.94−3.85 (m, 1H, $POCH_2$), 3.83−3.74 (m, 1H, $POCH_2$) 3.08 (d, ^2J(H,H) = 14.0 Hz, 1H, SCH_2), 2.88 (d, ^2J(H,H) = 13.9 Hz, 1H, SCH_2), 1.22 (t, ^3J(H,H) = 7.0 Hz, 3H, CH_3), 1.04 ppm (t, ^3J(H,H) = 7.0 Hz, 3H, CH_3). ^{13}C NMR (125.76 MHz, [D_6]DMSO): δ = 165.80 (C═O), 135.76 (d, ^2J(C,P) = 4.3 Hz), 129.61 (d, ^3J(C,P) = 6.2 Hz), 128.71, 128.04 (d, ^5J(C,P) = 1.5 Hz), 63.04 (d, ^2J(C,P) = 7.3 Hz, $POCH_2$), 62.98 (d, ^2J(C,P) = 7.4 Hz, $POCH_2$), 44.39 (d, ^1J(C,P) = 143.9 Hz, PC), 31.83 (d, ^3J(C,P) = 6.5 Hz, SCH_2), 16.60 (d, ^3J(C,P) = 5.5 Hz, CH_3), 16.37 ppm (d, ^3J(C,P) = 5.5 Hz, CH_3). IR (NaCl): $\tilde{\nu}$ =3385 (s; ν(N−H)), 3192 (s; ν(O−H)), 2982 (s; ν(C−H_{aliph})), 2931 (s; ν(C−H_{aliph})), 1651 (s; ν(C═O)), 1240 (s; ν(P═O)), 1021 cm^{-1} (s; ν(P−O)). Elemental analysis calculated (%) for $C_{13}H_{20}NO_5PS$: C 46.84, H 6.05, N 4.20. Found: C 46.76, H 6.10, N 3.90.

Diethyl ((3,4-Difluorophenyl)((2-(hydroxyamino)-2-oxoethyl)thio)methyl)phosphonate (6b). White solid; yield 31% (1.141 g, 3.09 mmol); mp 105 °C. ^{1}H NMR (500.13 MHz, [D_6]DMSO): δ = 10.65 (br s, OH), 10.58 (br s, OH), 10.23 (br s, OH), 10.14 (br s, OH), 9.26 (br s, NH), 9.07 (br s, NH), 8.95 (br s, NH), 7.54−7.36 (m, 2H), 7.36−7.19 (m, 1H), 4.87 (d, ^2J(H,P) = 19.2 Hz, 0.12H, PCH), 4.67 (d, ^2J(H,P) = 20.5 Hz, 0.88H, PCH), 4.16−4.02 (m, 2H, $POCH_2$), 4.01−3.78 (m, 2H, $POCH_2$), 3.07 (d, ^2J(H,H) = 13.9 Hz, 1H, SCH_2), 2.92 (d, ^2J(H,H) = 13.9 Hz, 1H, SCH_2), 1.23 (t, ^3J(H,H) = 7.0 Hz, 3H, CH_3), 1.08 ppm (t, ^3J(H,H) = 7.0 Hz, 3H, CH_3). ^{13}C NMR (125.76 MHz, [D_6]DMSO): δ = 165.00 (C═O), 164.40 (C═O), 148.94 (dd, ^1J(C,F) = 244.6 Hz, ^2J(C,F) = 12.7 Hz), 148.78 (d, ^1J(C,F) = 246.6 Hz), 133.33 (m), 126.18 (m), 117.97 (dd, ^2J(C,F) = 18.0 Hz, ^3J(C,F) = ^3J(C,P) = 6.1 Hz), 117.40 (d, ^2J(C,F) = 17.0 Hz), 62.86 (d, ^2J(C,P) = 6.8 Hz, $POCH_2$), 62.75 (d, ^2J(C,P) = 6.8 Hz, $POCH_2$), 48.29 (d, ^1J(C,P) = 139.7 Hz, PC), 43.08 (d, ^1J(C,P) = 144.0 Hz, PC), 31.50 (d, ^3J(C,P) = 7.4 Hz, SCH_2), 16.16 (d, ^3J(C,P) = 5.5 Hz, CH_3), 15.97 ppm (d, ^3J(C,P) = 5.4 Hz, CH_3). IR (KBr): $\tilde{\nu}$ =3192 (s; ν(N−H), ν(O−H)), 2990 (s; ν(C−H_{aliph})), 2918 (s; ν(C−H_{aliph})), 1652 (s; ν(C═O)), 1236 (s; ν(P═O)), 1026 cm^{-1} (s; ν(P−O)). Elemental analysis calculated (%) for $C_{13}H_{16}F_2NO_5PS$: C 42.28, H 4.91, N 3.79. Found: C 42.08, H 4.82, N 3.86.

Diethyl ((3,4-Dichlorophenyl)((2-(hydroxyamino)-2-oxoethyl)thio)methyl)phosphonate (6c). Colorless oil; yield 38% (1.528 g, 3.80 mmol). ^{1}H NMR (500.13 MHz, [D_6]DMSO): δ = 10.66 (br s, OH), 10.59 (br s, OH), 10.15 (br s, OH), 9.26 (br s, NH), 9.09−9.06 (m, NH), 8.99−8.90 (m, NH), 7.66 (d, J = 8.3 Hz, 1H), 7.64−7.58 (m, 1H), 7.46−7.36 (m, 1H), 4.91 (d, ^2J(H,P) = 19.3 Hz, 0.09H, PCH), 4.69 (d, ^2J(H,P) = 20.7 Hz, 0.91H, PCH), 4.16−4.02 (m, 2H, $POCH_2$), 3.98−3.81 (m, 2H, $POCH_2$), 3.06 (dd, ^2J(H,H) = 13.8 Hz, ^4J(H,P) = 1.4 Hz, 1H, SCH_2), 2.94 (d, ^2J(H,H) = 13.8 Hz, 1H, SCH_2), 1.23 (t, ^3J(H,H) = 7.0 Hz, 3H, CH_3), 1.09 ppm (t, ^3J(H,H) = 7.0 Hz, 3H, CH_3). ^{13}C NMR (125.76 MHz, [D_6]DMSO): δ = 164.86 (C═O), 136.87 (d, ^2J(C,P) = 4.1 Hz), 130.85 (d, ^3J(C,P) = 6.4 Hz), 130.78 (d, ^4J(C,P) = 1.3 Hz), 130.53 (d, ^5J(C,P) = 1.1 Hz), 130.26 (d, ^4J(C,P) = 3.0 Hz), 129.41 (d, ^3J(C,P) = 6.1 Hz), 62.93 (d, ^2J(C,P) = 6.7 Hz, $POCH_2$), 62.75 (d, ^2J(C,P) = 6.8 Hz, $POCH_2$), 42.98 (d, ^1J(C,P) = 143.4 Hz, PC), 31.57 (d, ^3J(C,P) = 7.5 Hz, SCH_2), 16.15 (d, ^3J(C,P) = 5.5 Hz, CH_3), 15.96 ppm (d, ^3J(C,P) = 5.5 Hz, CH_3). IR (NaCl): $\tilde{\nu}$ =3190 (s; ν(N−H), ν(O−H)), 2985 (s; ν(C−H_{aliph})), 2910 (s; ν(C−H_{aliph})), 1661 (s; ν(C═O)), 1239 (s; ν(P═O)), 1024 cm^{-1} (s; ν(P−O)). Elemental analysis calculated (%) for $C_{13}H_{18}Cl_2NO_5PS$: C 38.82, H 4.51, N 3.48. Found: C 39.10, H 4.69, N 3.42.

General Procedure for the Synthesis of Compounds 5a−e and 7a−c. The appropriate phosphonic acid diethyl ester **4a−e**, **6a−c** (1equiv, 1 mmol) was dissolved in dry dichloromethane (10 mL) under an atmosphere of nitrogen. The solution was cooled to 0 °C, and trimethylsilyl bromide (5 equiv, 0.66 mL, 5 mmol) was added dropwise via a syringe. After being stirred for 1 h, the reaction mixture was allowed to warm to room temperature and was stirred for further 47 h. The solvent was removed under reduced pressure, and tetrahydrofuran (10 mL) was added to the residue. The solution was treated with water (3 equiv, 0.05 mL, 3 mmol) and the reaction mixture was stirred for 45 min at room temperature. The solvent was evaporated and the residue was dried in vacuo overnight. Addition of ethyl acetate afforded phosphonic acids **5a−e** as white solids. Target compounds **7a−c** were obtained as colorless oils after purification of the crude products by filtration through a small amount of silica gel using ethyl acetate as the eluent. ^{1}H and ^{13}C NMR spectra for compounds **5a−e** and **7a−c** are provided in Figures S7−S22.

(((2-(Hydroxy(methyl)amino)-2-oxoethyl)thio)(phenyl)-methyl)phosphonic Acid (5a). White solid; yield 38% (0.111 g, 0.38 mmol); mp 112 °C. ^{1}H NMR (500.13 MHz, [D_6]DMSO): δ = 9.99 (br s, OH), 7.47−7.35 (m, 2H), 7.34−7.26 (m, 2H), 7.26−7.18 (m, 1H), 4.25 (d, ^2J(H,P) = 19.0 Hz, 1H, PCH), 3.50 (d, ^2J(H,H) = 14.6 Hz, 1H, SCH_2), 3.23 (d, ^2J(H,H) = 14.6 Hz, 1H, SCH_2), 3.06 (s, 3H, NCH_3). ^{13}C NMR (125.76 MHz, [D_6]DMSO): δ = 168.93 (C═O), 137.36 (d, ^2J(C,P) = 3.8 Hz), 129.23 (d, ^3J(C,P) = 5.8 Hz), 127.86, 126.78, 45.72 (d, ^1J(C,P) = 139.2 Hz, PC), 35.71 (NCH_3), 31.85 (d, ^3J(C,P) = 6.2 Hz, SCH_2). IR (KBr): $\tilde{\nu}$ =3192 (s; ν(O−H)), 2925 (s; ν(C−H_{aliph})), 1630 (s; ν(C═O)), 1191 (s; ν(P═O)), 987 cm^{-1} (s; ν(P−O)). HRMS (ESI): m/z calculated for $C_{10}H_{14}NO_5PS$ + H^+ [M + H^+]: 292.040 31. Found: 292.039 87. HPLC analysis: retention time = 1.870 min; peak area, 99.08%; eluent A, NH_4OAc solution (5 mM); eluent B, CH_3CN; isocratic (1:1) over 20 min with a flow rate of 1 mL min^{-1}.

(*R*)-**5a**: $[\alpha]_D^{20}$ −80.67 deg cm^3 g^{-1} dm^{-1} (c 0.011 g cm^{-3} in methanol with 0.1% trifluoroacetic acid).

(*S*)-**5a**: $[\alpha]_D^{20}$ +80.53 deg cm^3 g^{-1} dm^{-1} (c 0.001 g cm^{-3} in methanol with 0.1% trifluoroacetic acid).

dx.doi.org/10.1021/jm4012559 | J. Med. Chem. XXXX, XXX, XXX−XXX

((3,4-Difluorophenyl)((2-(hydroxy(methyl)amino)-2-oxoethyl)thio)methyl)phosphonic Acid (5b). White solid; yield 45% (0.15 g, 0.46 mmol); mp 137 °C. ^{1}H NMR (500.13 MHz, [D$_6$]DMSO): δ = 10.04 (br s, OH), 7.51−7.31 (m, 2H), 7.28−7.14 (m, 1H), 4.28 (d, ^2J(H,P) = 19.6 Hz, 0.83H, PCH), 4.21 (d, ^2J(H,P) = 19.2 Hz, 0.17H, PCH), 3.46 (d, ^2J(H,H) = 14.6 Hz, 1H, SCH$_2$), 3.23 (d, ^2J(H,H) = 14.6 Hz, 1H, SCH$_2$), 3.09 (s, 0.21H, NCH$_3$), 3.05 (s, 2.54H, NCH$_3$), 3.01 ppm (s, 0.25H, NCH$_3$). ^{13}C NMR (125.76 MHz, [D$_6$]DMSO): δ = 168.66 (C═O), 148.79 (dd, ^1J(C,F) = 244.7 Hz, ^2J(C,F) = 11.7 Hz), 148.34 (dd, ^1J(C,F) = 244.8 Hz, ^2J(C,F) = 12.5 Hz), 135.58, 126.12 (m), 117.80 (dd, ^2J(C,F) = 17.7 Hz, ^3J(C,F) = ^3J(C,P) = 5.6 Hz), 116.77 (d, ^2J(C,F) = 17.0 Hz), 45.01 (d, ^1J(C,P) = 137.8 Hz, PC), 35.70 (NCH$_3$), 31.88 ppm (d, ^3J(C,P) = 7.4 Hz, SCH$_2$). IR (KBr): $\tilde{\nu}$ =3162 (s; ν(O−H)), 2925 (s; ν(C−H$_{aliph}$)), 1609 (s; ν(C═O)), 1196 (s; ν(P═O)), 988 cm^{-1} (s; ν(P−O)). Elemental analysis calculated (%) for $C_{10}H_{12}F_2NO_5PS$: C 36.70, H 3.70, N 4.28, found: C 36.97, H 4.00, N 3.92.

((3,4-Dichlorophenyl)((2-(hydroxy(methyl)amino)-2-oxoethyl)thio)methyl)phosphonic Acid (5c). White solid; yield 45% (0.162 g, 0.45 mmol); mp 134 °C. ^{1}H NMR (500.13 MHz, [D$_6$]DMSO): δ = 10.01 (br s, OH), 7.70−7.52 (m, 2H), 7.45−7.30 (m, 1H), 4.32 (d, ^2J(H,P) = 19.8 Hz, 0.86H, PCH), 4.24 (d, ^2J(H,P) = 19.8 Hz, 0.14H, PCH), 3.47 (d, ^2J(H,H) = 14.6 Hz, 1H, SCH$_2$), 3.25 (d, ^2J(H,H) = 14.6 Hz, 1H, SCH$_2$), 3.12−2.97 ppm (m, 3H, NCH$_3$). ^{13}C NMR (125.76 MHz, [D$_6$]DMSO): δ = 168.55 (C═O), 138.99 (m), 130.84 (d, ^3J(C,P) = 5.8 Hz), 130.42 (d, ^4J(C,P) = 1.3 Hz), 130.07, 129.63 (d, ^3J(C,P) = 5.8 Hz), 129.42 (d, ^4J(C,P) = 2.3 Hz), 44.85 (d, ^1J(C,P) = 137.3 Hz, PC), 35.71 (NCH$_3$), 31.96 ppm (d, ^3J(C,P) = 7.4 Hz, SCH$_2$). IR (KBr): $\tilde{\nu}$ =3175 (s; ν(O−H)), 2923 (s; ν(C−H$_{aliph}$)), 1618 (s; ν(C═O)), 1191 (s; ν(P═O)), 984 cm^{-1} (s; ν(P−O)). Elemental analysis calculated (%) for $C_{10}H_{12}Cl_2NO_5PS$: C 33.35, H 3.36, N 3.89. Found: C 33.06, H 3.47, N 3.63.

(((2-(Hydroxy(methyl)amino-2-oxoethyl)thio)(naphthalen-1-yl)methyl)phosphonic Acid (5d). White solid; yield 55% (0.188 g, 0.55 mmol); mp 137 °C. ^{1}H NMR (500.13 MHz, [D$_6$]DMSO): δ = 9.99 (br s, OH), 8.20 (d, J = 6.9 Hz, 1H), 7.92 (d, J = 7.9 Hz, 1H), 7.88 (s, 1H), 7.83 (d, J = 8.1 Hz, 1H), 7.59−7.44 (m, 3H), 5.19 (d, ^2J(H,P) = 18.3 Hz, 1H, PCH), 3.74 (d, ^2J(H,H) = 14.2 Hz, 1H, SCH$_2$), 3.34 (d, ^2J(H,H) = 14.5 Hz, 1H, SCH$_2$), 3.05 ppm (s, 3H, NCH$_3$). ^{13}C NMR (125.76 MHz, [D$_6$]DMSO): δ = 169.11 (C═O), 133.55 (m), 133.26 (m), 131.28 (m), 128.46, 127.36, 126.95 (m), 126.00 (m), 125.47, 125.22, 123.61, 38.61 (m, PC), 35.72 (NCH$_3$), 32.34 ppm (m, SCH$_2$). IR (KBr): $\tilde{\nu}$ =3225 (s; ν(O−H)), 2928 (s; ν(C−H$_{aliph}$)), 1596 (s; ν(C═O)), 1132 (s; ν(P═O)), 1021 cm^{-1} (s; ν(P−O)). HRMS (ESI): m/z calculated for $C_{14}H_{16}NO_5PS + H^+$ [M + H$^+$]: 342.055 96. Found: 342.055 37. HPLC analysis: retention time = 1.860 min; peak area, 99.39%; eluent A, NH$_4$OAc solution (5 mM); eluent B, CH$_3$CN; isocratic (1:1) over 20 min with a flow rate of 1 mL min^{-1} and detection at 254 nm; column temperature, rt.

(((2-(Hydroxy(methyl)amino)-2-oxoethyl)thio)(*p*-tolyl)-methyl)phosphonic Acid (5e). White solid; yield 36% (0.110 g, 0.36 mmol); mp 100 °C. ^{1}H NMR (500.13 MHz, [D$_6$]DMSO): δ = 10.92 (br s, OH), 10.03 (br s, OH), 7.27 (d, ^3J(H,H) = 7.9 Hz, 2H), 7.10 (d, ^3J(H,H) = 7.8 Hz, 2H), 4.19 (d, ^2J(H,P) = 18.9 Hz, 0.86H, PCH), 4.10 (d, ^2J(H,P) = 19.1 Hz, 0.14H, PCH), 3.48 (d, ^2J(H,H) = 14.6 Hz, 1H, SCH$_2$), 3.20 (d, ^2J(H,H) = 14.6 Hz, 1H, SCH$_2$), 3.12−2.99 (m, 3H, NCH$_3$), 2.34−2.21 (m, 3H, CH$_{3arom}$). ^{13}C NMR (125.76 MHz, [D$_6$]DMSO): δ = 168.99 (C═O), 135.87, 134.32 (m), 129.13 (d, ^3J(C,P) = 5.7 Hz), 128.44, 45.46 (d, ^1J(C,P) = 139.5 Hz, PC), 35.71 (NCH$_3$), 31.79 (m, SCH$_2$), 20.60 (CH$_{3arom}$). IR (KBr): $\tilde{\nu}$ =3116 (s; ν(O−H)), 3011 (s; ν(C−H$_{aliph}$)), 2928 (s; ν(C−H$_{aliph}$)), 1625 (s; ν(C═O)), 1190 (s; ν(P═O)), 986 cm^{-1} (s; ν(P−O)). HRMS (ESI): m/z calculated for $C_{11}H_{16}NO_5PS - H^+$ [M − H$^+$]: 304.041 40. Found: 304.041 65. HPLC analysis: retention time = 2.753 min; peak area, 95.72%; eluent, CH$_3$CN; 20 min with a flow rate of 1 mL min^{-1} and detection at 254 nm; column temperature, rt.

(((2-(Hydroxyamino)-2-oxoethyl)thio)(phenyl)methyl)-phosphonic Acid (7a). Colorless oil; yield 61% (0.169 g, 0.61 mmol). ^{1}H NMR (500.13 MHz, [D$_6$]DMSO): δ = 10.61 (br s, NOH), 10.17 (br s, NH), 7.47−7.18 (m, 5H), 6.41 (br, s, POH), 4.33 (d, ^2J(H,P) = 18.9 Hz, 0.84, PCH), 4.18 (d, ^2J(H,P) = 18.8 Hz, 0.16H, PCH), 3.47−3.36 (m, 0.11H, SCH$_2$), 3.29 (d, ^2J(H,H) = 14.8 Hz, 0.11H, SCH$_2$), 3.08 (d, ^2J(H,H) = 13.9 Hz, 0.85H, SCH$_2$), 3.00 (d, ^2J(H,H) = 14.9 Hz, 0.18H, SCH$_2$), 2.81 (d, ^2J(H,H) = 13.9 Hz, 0.75H, SCH$_2$). ^{13}C NMR (125.76 MHz, [D$_6$]DMSO): δ = 165.95 (C═O), 137.17 (d, ^2J(C,P) = 4.3 Hz), 129.33 (d, ^3J(C,P) = 5.8 Hz), 127.99, 126.95, 46.20 (d, ^1J(C,P) = 139.2 Hz, PC), 31.48 (d, ^3J(C,P) = 6.1 Hz, SCH$_2$). IR (NaCl): $\tilde{\nu}$ =3457 (s; ν(N−H)), 3155 (s; ν(O−H)), 3001 (s; ν(C−H$_{aliph}$)), 1653 (s; ν(C═O)), 1161 (s; ν(P═O)), 1006 cm^{-1} (s; ν(P−O)). HRMS (ESI): m/z calculated for $C_9H_{12}NO_5PS - H^+$ [M − H$^+$]: 276.010 10. Found: 276.010 106. HPLC analysis: retention time = 1.850 min; peak area, 99.82%; eluent A, NH$_4$OAc solution (5 mM); eluent B, CH$_3$CN; isocratic (1:1) over 20 min with a flow rate of 1 mL min^{-1} and detection at 254 nm; column temperature, rt.

((3,4-Difluorophenyl)((2-(hydroxyamino)-2-oxoethyl)thio)-methyl)phosphonic Acid (7b). Colorless oil; yield 42% (0.132 g, 0.42 mmol). ^{1}H NMR (500.13 MHz, [D$_6$]DMSO): δ = 10.57 (br s, NOH), 9.00 (br s, NH, POH), 7.63−7.09 (m, 3H), 4.46 (d, ^2J(H,P) = 19.1 Hz, 0.09H, PCH), 4.36 (d, ^2J(H,P) = 19.6 Hz, 0.59H, PCH), 4.23 (d, ^2J(H,P) = 19.5 Hz, 0.32H, PCH), 3.76−3.62 (m, 0.02H, SCH$_2$), 3.62−3.46 (m, 0.06H, SCH$_2$), 3.45−3.06 (m, 0.92H, SCH$_2$), 13.02 (d, ^2J(H,H) = 13.8 Hz, 0.52H, SCH$_2$), 2.81 ppm (d, ^2J(H,H) = 13.8 Hz, 0.48H, SCH$_2$). ^{13}C NMR (125.76 MHz, [D$_6$]DMSO): δ = 165.53 (C═O), 148.85 (dd, ^1J(C,F) = 244.5 Hz, ^2J(C,F) = 12.2 Hz), 148.47 (dd, ^1J(C,F) = 245.6 Hz, ^2J(C,F) = 11.4 Hz), 135.09 (m), 126.20, 117.88 (dd, ^2J(C,F) = 17.5 Hz, ^3J(C,F) = ^3J(C,P) = 4.5 Hz), 116.88 (d, ^2J(C,F) = 17.1 Hz), 45.40 (d, ^1J(C,P) = 137.9 Hz, PC), 45.31 (d, ^1J(C,P) = 137.8 Hz, PC), 33.27 (d, ^3J(C,P) = 7.5 Hz, SCH$_2$), 31.35 ppm (d, ^3J(C,P) = 7.1 Hz, SCH$_2$). IR (NaCl): $\tilde{\nu}$ =3418 (s; ν(N−H)), 3154 (s; ν(O−H)), 3001 (s; ν(C−H$_{aliph}$)), 2926 (s; ν(C−H$_{aliph}$)), 1653 (s; ν(C═O)), 1119 (s; ν(P═O)), 1006 cm^{-1} (s; ν(P−O)). HRMS (ESI): m/z calculated for $C_9H_{10}F_2NO_5PS + H^+$ [M + H$^+$]: 314.005 81. Found: 314.006 21. HPLC analysis: retention time = 1.790 min; peak area, 99.76%; eluent A, NH$_4$OAc solution (5 mM); eluent B, CH$_3$CN; isocratic (1:1) over 20 min with a flow rate of 1 mL min^{-1} and detection at 254 nm; column temperature, rt.

((3,4-Dichlorophenyl)((2-(hydroxyamino)-2-oxoethyl)thio)-methyl)phosphonic Acid (7c). Colorless oil; yield 44% (0.152 g, 0.44 mmol). ^{1}H NMR (500.13 MHz, [D$_6$]DMSO): δ = 10.57 (br s, NOH), 10.06 (br s, NOH), 9.26 (br s, NH, POH), 8.98 (br s, NH, POH), 7.71−7.48 (m, 2H), 7.45−7.24 (m, 1H), 4.51 (d, ^2J(H,P) = 19.0 Hz, 0.06H, PCH), 4.37 (d, ^2J(H,P) = 19.8 Hz, 0.6H, PCH), 4.24 (d, ^2J(H,P) = 19.9 Hz, 0.34H, PCH), 3.71−3.48 (m, 0,28H, SCH$_2$), 3.48−3.32 (m, 0.26H, SCH$_2$), 3.31−3.06 (m, 0.55H, SCH$_2$), 3.02 (d, ^2J(H,H) = 13.8 Hz, 0.47H, SCH$_2$), 2.82 (d, ^2J(H,H) = 13.9 Hz, 0.44H, SCH$_2$). ^{13}C NMR (125.76 MHz, [D$_6$]DMSO): δ = 165.42 (C═O), 138.78 (d, ^2J(C,P) = 4.2 Hz), 130.89 (d, ^3J(C,P) = 5.9 Hz), 130.48 (d, ^4J(C,P) = 1.1 Hz), 130.12, 129.67 (d, ^3J(C,P) = 5.7 Hz), 129.51 (d, ^4J(C,P) = 2.7 Hz), 45.63 (d, ^1J(C,P) = 137.1 Hz, PC), 45.36 (d, ^1J(C,P) = 137.0 Hz, PC), 31.37 (d, ^3J(C,P) = 7.7 Hz, SCH$_2$). IR (NaCl): $\tilde{\nu}$ = 3192 (s; ν(N−H), ν(O−H)), 2978 (s; ν(C−H$_{aliph}$)), 1651 (s; ν(C═O)), 1134 (s; ν(P═O)), 1028 cm^{-1} (s; ν(P−O)). HRMS (ESI): m/z calculated for $C_9H_{10}Cl_2NO_5PS - H^+$ [M − H$^+$]: 343.932 16. Found: 343.932 51. HPLC analysis: retention time = 1.823 min; peak area, 99.95%; eluent A, NH$_4$OAc solution (5 mM); eluent B, CH$_3$CN; isocratic (1:1) over 20 min with a flow rate of 1 mL min^{-1} and detection at 254 nm; column temperature, rt.

Biological Evaluation. Gene Expression and Protein Purification. The recombinant *E. coli* strain M15 pREP4 pQEIspCplasart[20] was grown to an optical density of 0.6 at 37 °C in LB medium supplemented with ampicillin (180 mg L^{-1}) and kanamycin (50 mg L^{-1}). Isopropylthiogalactoside was added to a final concentration of 1 mM, and the cell suspension was cultivated overnight at 30 °C under shaking (120 rpm). Cells were harvested by centrifugation, washed with 0.9% NaCl solution, and resuspended in loading buffer (100 mM Tris hydrochloride, pH 7.4, containing 0.5 M NaCl and 20 mM imidazole). The suspension was passed through a cell disruption device (basic Z model, Constant Systems Limited, Northamptonshire, U.K.) and was then centrifuged. The supernatant was subjected to a

Ni^{2+}-chelating Sepharose fast flow column (volume of 40 mL) that had been pre-equilibrated with loading buffer. The column was flushed with 100 mM Tris hydrochloride, pH 7.4, containing 0.5 M NaCl and 100 mM imidazole to remove unbound protein and was then developed with 100 mM Tris hydrochloride, pH 7.4, containing 0.5 M NaCl and 250 mM imidazole. Fractions were combined and dialyzed overnight against 50 mM Tris hydrochloride, pH 7.4, containing 2 mM DTT and 0.02% NaN_3. *Pf*IspC was obtained with approximately 95% purity, as estimated by SDS−PAGE analysis.

IC_{50} Determination Using the Photometric Assay. Assays were conducted in 96-well plates (Nunc, catalog no. 781602) with transparent flat bottoms. Assay mixtures (total volume of 200 μL) contained 100 mM Tris hydrochloride, pH 7.6, 5 mM $MgCl_2$, 5 mM DTT, 0.5 mM NADPH, 0.02 U of IspC protein, and test compounds. Dilution series (1:3) of inhibitors approximately covered the concentration range of 200−0.003 μM. The reaction was started by addition of 1-deoxy-D-xylulose 5-phosphate in 100 mM Tris hydrochloride, pH 8.0, to a final concentration of 0.5−5.0 mM. The reaction was monitored photometrically (room temperature) at 340 nm using a plate reader (SpectraMax M5, Molecular Devices, Biberach an der Riss, Germany). IC_{50} values (mean ± standard deviation calculated from eight or more measuring points) were determined using nonlinear regression analysis as described earlier.[41,42] The IC_{50} values are provided in Tables 1 and 3.

In Vitro Drug Sensitivity Assay. The chloroquine sensitive *P. falciparum* laboratory strain 3D7 and the chloroquine-resistant strain Dd2 were kept in continuous culture as described previously.[43] In brief, parasites were kept in an incubator at 37 °C in an atmosphere of 5% CO_2 and 5% oxygen at 5% hematocrit in erythrocytes of blood group 0 rhesus + in complete culture medium (RPMI 1640, 25 mM 4-(2-hydroxyethyl)piperazine-*N*′-(4-butanesulfonic acid), 2 mM L-glutamine, 50 μg mL^{-1} gentamycin, and 0.5% w/v albumax) with daily change of medium. Synchronization of parasite culture was performed by sorbitol.[44]

Tested compounds were dissolved in DMSO at stock concentrations between 25 and 100 mM, and further dilutions were done with complete culture medium. Final concentrations of solvent did not interfere with parasite growth (data not shown).

Activity of compounds was evaluated in a drug sensitivity assay by measurement of histidine rich protein 2 (HRP2) with an enzyme-linked immunsorbent assay (ELISA) according to standard procedures.[45] In brief, 96-well plates were precoated with a 3-fold dilution of the respective compound before adding ring stage parasites at a parasitemia of 0.05% and a hematocrit of 1.5% in a total volume of 225 μL per well. After an incubation time of 3 days plates were freeze−thawed twice before performance of HRP2-ELISA. As internal control chloroquine was evaluated in each assay. Experiments were performed in duplicate.

Statistics. The 50% inhibitory concentrations (IC_{50}) was determined by analyzing the log of the concentration−response curves by nonlinear regression analysis using the drc-package, version 0.9.0, of R, version 2.10.1 (R Development Core Team).[46] The IC_{50} values are provided in Table 2.

Crystallization and Structure Determination. *Pf*IspC protein (11 mg mL^{-1} in 50 mM Tris hydrochloride, pH 7.4, containing 2 mM DTT and 0.02% NaN_3) was incubated with 1.5 mM **5a** (racemate), 640 μM $MnCl_2$, and 800 μM NADPH prior to crystallization. Crystals were prepared by using the sitting drop vapor diffusion method at 20 °C. The droplets comprised 0.1 μL of protein and 0.1 μL of reservoir solution (2% PEG4000, 100 mM Na acetate, and 15% MPD, pH 5.0). Crystals grew to a final size of 500 × 100 × 50 μm^3 within 6 weeks. *Pf*IspC cocrystals were supercooled without further cryoprotectant in a stream of nitrogen gas at 100 K (Oxford Cryo Systems). A native data set at 2.0 Å resolution was collected using synchrotron radiation at the X06SA beamline, Swiss Light Source, Villigen, Switzerland. Data were processed using the program package XDS,[47] and data reduction was performed with XSCALE with a final R_{free} value of 24.9% and root-mean-square deviation (rmsd) bond and angle values of 0.09 Å and 1.2°, respectively (Table 4). Crystal structure analysis was carried out by molecular replacement using coordinates of *Pf*IspC deposited at the Protein Data Bank (PDB code 3AU8[37]). The anisotropy of diffraction was corrected by TLS refinement using the program REFMAC5.[48] Conventional crystallographic rigid body, positional, and temperature factor refinements were calculated with REFMAC5. The model was completed using the interactive three-dimensional graphic program MAIN.[49] The atomic coordinates for *Pf*IspC in complex with *S*-**5a**, Mn^{2+}, and NADPH have been deposited in the Protein Data Bank, Research Collaboratory for Structural Bioinformatics at Rutgers University, under the accession code 4KP7.

Table 4. Data Collection and Refinement Statistics

	S-**5a**/*Pf*IspC/Mn/NADPH
	Crystal Parameter
space group	$P2_1$
cell dimensions	a = 51.5 Å, b = 78.1 Å, c = 100.0 Å; β = 91.5°
molecules per AU[a]	2
	Data Collection
beamline	SLS, X06SA
wavelength (Å)	1.0
resolution range (Å)[b]	40−2.0 (2.1−2.0)
observed/unique[c] reflections	196791/52039
completeness (%)[b]	97.1 (96.7)
R_{merge} (%)[b,d]	8.2 (53.3)
$I/\sigma(I)$ [b]	12.7 (3.0)
	Refinement
resolution (Å)	15−2.0
R_{work}/R_{free} [e]	18.5/24.9
no. atoms	6790
protein	6468
ligand	84
Mn^{2+}	2
water	236
B-factors	37.0
rmsd[f]	
bond length (Å)	0.009
bond angle (deg)	1.20
Ramachandran (%)[g]	97.3/2.7/0.0
PDB accession code	4KP7

[a]Asymmetric unit. [b]Values in parentheses of resolution range, completeness, R_{merge}, and $I/\sigma(I)$ correspond to the last resolution shell. [c]Friedel pairs were treated as identical reflections. [d]$R_{merge}(I) = \sum_{hkl}\sum_j|[I(hkl)_j - I(hkl)]|/\sum_{hkl}I_{hkl}$, where $I(hkl)_j$ is the measurement of the intensity of reflection hkl and $\langle I(hkl)\rangle$ is the average intensity. [e]$R = \sum_{hkl}||F_{obs}| - |F_{calc}||/\sum_{hkl}|F_{obs}|$, where R_{free} is calculated without a σ cutoff for a randomly chosen 5% of reflections, which were not used for structure refinement, and R_{work} is calculated for the remaining reflections. [f]Root mean square deviations from ideal bond lengths/angles. [g]Number of residues in favored region/allowed region/outlier region.

LC−MS System. LC−MS analysis was performed with an Agilent (Santa Clara, CA, USA) 1200 HPLC system consisting of a binary pump (G1312B), cooled autosampler (G1367D), thermostated column compartment (G1316), and degasser (G1379B) coupled to an ABSciex (Framingham, MA, USA) API4000 mass spectrometer equipped with a Turbo V IonSpray source (electrospray ionization) equipped with a reversed phase Phenomenex Synergy C_{12} column (150 mm × 2 mm, 4 μm, 80 Å). Samples were chromatographed isocratically using water/methanol (3:1 v/v) with 0.1% formic acid, at 0.2 mL min^{-1}. The retention volume for the **5a** racemate as well as for each enantiomer was 0.74 mL. Data were acquired and analyzed using ABSciex "Analyst" software (version 1.6.2, Framingham, MA, USA).

Identification and Evaluation of Compound 5a Enantiomers 1 and 2. Mass spectra of enantiomers were obtained using the API4000 in multiple-reaction-monitoring (MRM) mode. The precursor ion with m/z value of 290 (negative mode) and its diagnostic product ions were defined using an automatic compound

dx.doi.org/10.1021/jm4012559 | J. Med. Chem. XXXX, XXX, XXX−XXX

optimization algorithm. MRM parameters are shown in Supporting Information Table S1. Peak identification was performed by comparison of retention times and usage of 5-MRM-transitions (Supporting Information Figure S6). The concentration of enantiomers 1 and 2 in stock solution was determined using peak integration of the most intensive MRM transition (m/z 243). The original **5a** sample (racemic mixture) was used as an external standard.

Polarimetry. Optical rotation was measured using a P8000 polarimeter from Krüss Optronic GmbH (Hamburg, Germany). Measurements were performed at 20 °C. The solvent was methanol containing 0.1% trifluoroacetic acid.

■ ASSOCIATED CONTENT

Supporting Information

Additional figures illustrating inhibition data, superpositions, and alignment of IspC from different organisms, details of multiple reaction monitoring, and NMR spectra. This material is available free of charge via the Internet at http://pubs.acs.org.

Accession Codes

PDB code for *Pf*IspC with bound **5a** is 4KP7.

■ AUTHOR INFORMATION

Corresponding Author

*E-mail: thomas.kurz@uni-duesseldorf.de. Phone: (+49)21181-14984. Fax: (+49)21181-13847.

Author Contributions

#A.K. and C.L. contributed equally.

Notes

The authors declare no competing financial interest.

■ ACKNOWLEDGMENTS

The Deutsche Forschungsgemeinschaft (DFG) is acknowledged for funds used to purchase the UHR-TOF maXis 4G, Bruker Daltonics HRMS instrument used in this research. We thank the staff of the beamline X06SA at the Paul Scherrer Institute, Swiss Light Source, Villigen, Switzerland, for their help with data collection.

■ ABBREVIATIONS USED

br s, broad signal; *n*-BuLi, *n*-butyllithium; DMAPP, dimethylallyl pyrophosphate; DMF, *N*,*N*-dimethylformamide; DMSO, dimethyl sulfoxide; DOXP, 1-deoxy-D-xylulose 5-phosphate; Dxr (IspC), 1-deoxy-D-xylulose 5-phosphate reductoisomerase; ee, enantiomeric excess; IPP, isopentenyl pyrophosphate; MEP, 2*C*-methyl-D-erythritol 4-phosphate; mp, melting point; NADPH, nicotinamide adenine dinucleotide phosphate; rt, room temperature; S, sulfur; THF, tetrahydrofuran; TMSBr, trimethylsilyl bromide

■ REFERENCES

(1) Ershov, Y. V. 2-C-Methylerythritol phosphate pathway of isoprenoid biosynthesis as a target in identifying new antibiotics, herbicides, and immunomodulators: a review. *Appl. Biochem. Microbiol.* **2007**, *43*, 115−138.

(2) Murray, C. J. L.; Rosenfeld, L. C.; Lim, S. S.; Andrews, K. G.; Foreman, K. J.; Haring, D.; Fullman, N.; Naghavi, M.; Lozano, R.; Lopez, A. D. Global malaria mortality between 1980 and 2010: a systematic analysis. *Lancet* **2012**, *379*, 413−431.

(3) Mordmüller, B.; Kremsner, P. G. Malarial parasites vs. antimalarials: never-ending rumble in the jungle. *Curr. Mol. Med.* **2006**, *6*, 247−251.

(4) Wells, T. N.; Poll, E. M. When is enough enough? The need for a robust pipeline of high-quality antimalarials. *Discovery Med.* **2010**, *9*, 389−398.

(5) Okuhara, M.; Kuroda, Y.; Goto, T.; Okamoto, M.; Terano, H.; Kohsaka, M.; Aoki, H.; Imanaka, H. Studies on new phosphonic acid antibiotics. 3. Isolation and characterization of FR-31564, FR-32863 and FR-33289. *J. Antibiot.* **1980**, *33*, 24−28.

(6) Kuroda, Y.; Okuhara, M.; Goto, T.; Okamoto, M.; Terano, H.; Kohsaka, M.; Aoki, H.; Imanaka, H. Studies on new phosphonic acid antibiotics. 4. Structure determination of FR-33289, FR-31564 and FR-32863. *J. Antibiot.* **1980**, *33*, 29−35.

(7) Jomaa, H.; Wiesner, J.; Sanderbrand, S.; Altincicek, B.; Weidemeyer, C.; Hintz, M.; Turbachova, I.; Eberl, M.; Zeidler, J.; Lichtenthaler, H. K.; Soldati, D.; Beck, E. Inhibitors of the nonmevalonate pathway of isoprenoid biosynthesis as antimalarial drugs. *Science* **1999**, *285*, 1573−1576.

(8) Singh, N.; Cheve, G.; Avery, M. A.; McCurdy, C. R. Targeting the methyl erythritol phosphate (MEP) pathway for novel antimalarial, antibacterial and herbicidal drug discovery: inhibition of 1-deoxy-D-xylulose-5-phosphate reductoisomerase (DXR) enzyme. *Curr. Pharm. Des.* **2007**, *13*, 1161−1177.

(9) Rohmer, M.; Grosdemange-Billiard, C.; Seemann, M.; Tritsch, D. Isoprenoid biosynthesis as a novel target for antibacterial and antiparasitic drugs. *Curr. Opin. Invest. Drugs* **2004**, *5*, 154−162.

(10) Rohdich, F.; Bacher, A.; Eisenreich, W. Isoprenoid biosynthetic pathways as anti-infective drug targets. *Biochem. Soc. Trans.* **2005**, *33*, 785−791.

(11) Reichenberg, A.; Wiesner, J.; Weidemeyer, C.; Dreiseidler, E.; Sanderbrand, S.; Altincicek, B.; Beck, E.; Schlitzer, M.; Jomaa, H. Diaryl ester prodrugs of FR900098 with improved in vivo antimalarial activity. *Bioorg. Med. Chem. Lett.* **2001**, *11*, 833−835.

(12) Ortmann, R.; Wiesner, J.; Reichenberg, A.; Henschker, D.; Beck, E.; Jomaa, H.; Schlitzer, M. Alkoxycarbonyloxyethyl ester prodrugs of FR900098 with improved in vivo antimalarial activity. *Arch. Pharm.* **2005**, *338*, 305−314.

(13) Kurz, T.; Geffken, D.; Kaula, U.; Herbicidal/Pharmaceutical Composition Contains New and Known alpha-Substituted Organophosphorus Compound, Useful for Treating e.g. Viral, Bacterial or Protozoal Infections. International Patent Application DE/10356410-A1, WO/2005048715-A2, and WO/2005048715-A3, 2005; Bioagency AG.

(14) Kuntz, L.; Tritsch, D.; Grosdemange-Billiard, C.; Hemmerlin, A.; Willem, A.; Bacht, T. J.; Rohmer, M. Isoprenoid biosynthesis as a target for antibacterial and antiparasitic drugs: phosphonohydroxamic acids as inhibitors of deoxyxylulose phosphate reducto-isomerase. *Biochem. J.* **2005**, *386*, 127−135.

(15) Kurz, T.; Schlüter, K.; Kaula, U.; Bergmann, B.; Walter, R. D.; Geffken, D. Synthesis and antimalarial activity of chain substituted pivaloyloxymethyl ester analogues of fosmidomycin and FR900098. *Bioorg. Med. Chem.* **2006**, *14*, 5121−5135.

(16) Haemers, T.; Wiesner, J.; Van Poecke, S.; Goeman, J.; Henschker, D.; Beck, E.; Jomaa, H.; Van Calenbergh, S. Synthesis of α-substituted fosmidomycin analogues as highly potent *Plasmodium falciparum* growth inhibitors. *Bioorg. Med. Chem. Lett.* **2006**, *16*, 1888−1891.

(17) Schlüter, K.; Walter, R. D.; Bergmann, B.; Kurz, T. Arylmethyl substituted derivatives of fosmidomycin: synthesis and antimalarial activity. *Eur. J. Med. Chem.* **2006**, *41*, 1385−1397.

(18) Haemers, T.; Wiesner, J.; Giessmann, D.; Verbrugghen, T.; Hillaert, U.; Ortmann, R.; Jomaa, H.; Link, A.; Schlitzer, M.; Van Calenbergh, S. Synthesis of beta- and gamma-oxa isosteres of fosmidomycin and FR900098 as antimalarial candidates. *Bioorg. Med. Chem.* **2008**, *16*, 3361−3371.

(19) Verbrugghen, T.; Cos, P.; Maes, L.; Van Calenbergh, S. Synthesis and evaluation of α-halogenated analogues of 3-(acetylhydroxyamino)propylphosphonic acid (FR900098) as antimalarials. *J. Med. Chem.* **2010**, *53*, 5342−5346.

(20) Behrendt, C. T.; Kunfermann, A.; Illarionova, V.; Matheeussen, A.; Gräwert, T.; Groll, M.; Rohdich, F.; Bacher, A.; Eisenreich, W.; Fischer, M.; Maes, L.; Kurz, T. Synthesis and antiplasmodial activity of highly active reverse analogues of the antimalarial drug candidate fosmidomycin. *ChemMedChem* **2010**, *5*, 1673−1676.

(21) Behrendt, C. T.; Kunfermann, A.; Illarionova, V.; Matheeussen, A.; Pein, M. K.; Gräwert, T.; Kaiser, J.; Bacher, A.; Eisenreich, W.; Illarionov, B.; Fischer, M.; Maes, L.; Groll, M.; Kurz, T. Reverse fosmidomycin derivatives against the antimalarial drug target IspC (Dxr). *J. Med. Chem.* **2011**, *54*, 6796−6802.
(22) Andaloussi, M.; Henriksson, L. M.; Wieckowska, A.; Lindh, M.; Bjorkelid, C.; Larsson, A. M.; Suresh, S.; Iyer, H.; Srinivasa, B. R.; Bergfors, T.; Unge, T.; Mowbray, S. L.; Larhed, M.; Jones, T. A.; Karlén, A. Design, synthesis, and X-ray crystallographic studies of α-aryl substituted fosmidomycin analogues as inhibitors of *Mycobacterium tuberculosis* 1-deoxy-D-xylulose 5-phosphate reductoisomerase. *J. Med. Chem.* **2011**, *54*, 4964−4976.
(23) Kurz, T.; Behrendt, C.; Kaula, U.; Bergmann, B.; Walter, R. D. α-Phenylethyl substituted bis(pivaloyloxymethyl) ester analogues of fosmidomycin and FR900098. *Aust. J. Chem.* **2007**, *60*, 154−158.
(24) Behrendt, C. T. Synthese und Biologische Evaluation Inverser α-Aryl-Substituierter Fosmidomycin-Analoga. Ph.D. Thesis, Heinrich Heine Universität Düsseldorf, Germany, 2011.
(25) Brücher, K. Synthese und Biologische Evaluation von Inversen α-Substituierten, β-Oxa-Isosteren Fosmidomycin-Analoga und Derivaten mit Benzamid-Teilstruktur. Ph.D. Thesis, Heinrich Heine Universität Düsseldorf, Germany, 2012.
(26) Murakawa, T.; Sakamoto, H.; Fukada, S.; Konishi, T.; Nishida, M. Pharmakokinetics of fosmidomycin, a new phosphonic acid antibiotic. *Antimicrob. Agents Chemother.* **1982**, *21*, 224−230.
(27) Kuemmerle, H. P.; Murakawa, T.; Desantis, F. Pharmakokinetic evaluation of fosmidomycin, a new phosphonic acid antibiotic. *Chemioterapia* **1987**, *6*, 113−119.
(28) Borrmann, S.; Issifou, S.; Esser, G.; Adegnika, A. A.; Ramharter, M.; Matsiegui, P. B.; Oyakhirome, S.; Mawili-Mboumba, D. P.; Missinou, M. A.; Kun, J. F. J.; Jomaa, H.; Kremsner, P. G. Fosmidomycin-clindamycin for the treatment of *Plasmodium falciparum* malaria. *J. Infect. Dis.* **2004**, *190*, 1534−1540.
(29) Kappe, S. H. I.; Vaughan, A. M.; Boddey, J. A.; Cowman, A. F. That was then but this is now: malaria research in the time of an eradication agenda. *Science* **2010**, *328*, 862−866.
(30) Hoffman, R. V.; Nayyar, N. K. A facile preparation of *N*-(isopropoxyalkyl) amides by generation and trapping of *N*-acyliminium ions from ionization−rearrangement reactions of *N*-triflyloxy amides. *J. Org. Chem.* **1994**, *59*, 3530−3539.
(31) Casadei, M. A.; Dirienzo, B.; Inesi, A.; Moracci, F. M. Electrochemical studies on haloamides. 3. Haloacetamides and haloacetohydroxamates. *J. Chem. Soc., Perkin Trans. 1* **1992**, 375−378.
(32) Mikolajczyk, M.; Grzejszczak, S.; Chefczynska, A.; Zatorski, A. Organosulfur compounds. 23. Addition of elemental sulfur to phosphonate carbanions and its application for synthesis of α-phosphoryl organosulfur compounds: synthesis of aromatic ketones. *J. Org. Chem.* **1979**, *44*, 2967−2972.
(33) McKenna, C. E.; Higa, M. T.; Cheung, N. H.; McKenna, M. C. Facile dealkylation of phosphonic acid dialkyl esters by bromotrimethylsilane. *Tetrahedron Lett.* **1977**, 155−158.
(34) Leung, C. S.; Leung, S. S. F.; Tirado-Rives, J.; Jorgensen, W. L. Methyl effects on protein−ligand binding. *J. Med. Chem.* **2012**, *55*, 4489−4500.
(35) Brücher, K.; Illarionov, B.; Held, J.; Tschan, S.; Kunfermann, A.; Pein, M. K.; Bacher, A.; Gräwert, T.; Maes, L.; Mordmueller, B.; Fischer, M.; Kurz, T. α-Substituted β-oxa isosteres of fosmidomycin: synthesis and biological evaluation. *J. Med. Chem.* **2012**, *55*, 6566−6575.
(36) Kuzmic, P. Program DYNAFIT for the analysis of enzyme kinetic data: application to HIV proteinase. *Anal. Biochem.* **1996**, *237*, 260−273.
(37) Press, W. H.; Teukolsky, S. A.; Vetterling, W. T.; Flannery, B. P. *Numerical Recipes: The Art of Scientific Computing*, 3rd ed.; Cambridge University Press: New York, 2007.
(38) Botte, C. Y.; Dubar, F.; McFadden, G. I.; Marechal, E.; Biot, C. *Plasmodium falciparum* apicoplast drugs: targets or off-targets? *Chem. Rev.* **2012**, *112*, 1269−1283.
(39) Umeda, T.; Tanaka, N.; Kusakabe, Y.; Nakanishi, M.; Kitade, Y.; Nakamura, K. T. Molecular basis of fosmidomycin's action on the human malaria parasite *Plasmodium falciparum*. *Sci. Rep.* **2011**, 1−8.
(40) Steinbacher, S.; Kaiser, J.; Eisenreich, W.; Huber, R.; Bacher, A.; Rohdich, F. Structural basis of fosmidomycin action revealed by the complex with 2-C-methyl-D-erythritol 4-phosphate synthase (IspC). Implications for the catalytic mechanism and anti-malaria drug development. *J. Biol. Chem.* **2003**, *278*, 18401−18407.
(41) Deng, L.; Diao, J.; Chen, P.; Pujari, V.; Yao, Y.; Cheng, G.; Crick, D. C.; Prasad, B. V. V; Song, Y. Inhibition of 1-deoxy-D-xylulose-5-phosphate reductoisomerase by lipophilic phosphonates: SAR, QSAR, and crystallographic studies. *J. Med. Chem.* **2011**, *54*, 4721−4734.
(42) Creary, X.; Mehrsheikhmohammadi, M. E. The nature of cationic intermediates derived from α-thiophosphoryl and α-thiocarbonyl mesylates—neighboring thiophosphoryl and thiocarbonyl participation. *J. Org. Chem.* **1986**, *51*, 7−15.
(43) Trager, W.; Jensen, J. B. Human malaria parasites in continous culture. *Science* **1976**, *193*, 673−675.
(44) Lambros, C.; Vanderberg, J. P. Synchronization of *Plasmodium-falciparum* erythrocytic stages in culture. *J. Parasitol.* **1979**, *65*, 418−420.
(45) Noedl, H.; Bronnert, J.; Yingyuen, K.; Herwig, B. A.; Attlmayr, B.; Kollaritsch, H.; Fukuda, M. Simple histidine-rich protein 2 double-site sandwich enzyme-linked immunosorbent assay for use in malaria drug sensitivity testing. *Antimicrob. Agents Chemother.* **2005**, *49*, 3575−3577.
(46) R Development Core Team. *R: A Language and Environment for Statistical Computing*; R Foundation for Statistical Computing: Vienna, Austria, 2009.
(47) Kabsch, W. Automatic processing of rotation diffraction data from crystals of initially unknown symmetry and cell constants. *J. Appl. Crystallogr.* **1993**, *26*, 795−800.
(48) Murshudov, G. N.; Vagin, A. A.; Dodson, E. J. Refinement of macromolecular structures by the maximum-likelihood method. *Acta Crystallogr., Sect. D: Biol. Crystallogr.* **1997**, *53*, 240−255.
(49) Turk, D. Development and Usage of a Molecular Graphics Program. Ph.D. Thesis, Technische Universität München, Germany, 1992.